isvr Institute of Sound and Vibration Research

An Overview of the Single Degree of Freedom System and Zener Model for Passive Shock Isolation

D.F. Ledezma-Ramirez, N.S. Ferguson and M.J. Brennan

ISVR Technical Memorandum No 947

June 2005

University of Southampton

SCIENTIFIC PUBLICATIONS BY THE ISVR

Technical Reports are published to promote timely dissemination of research results by ISVR personnel. This medium permits more detailed presentation than is usually acceptable for scientific journals. Responsibility for both the content and any opinions expressed rests entirely with the author(s).

Technical Memoranda are produced to enable the early or preliminary release of information by ISVR personnel where such release is deemed to the appropriate. Information contained in these memoranda may be incomplete, or form part of a continuing programme; this should be borne in mind when using or quoting from these documents.

Contract Reports are produced to record the results of scientific work carried out for sponsors, under contract. The ISVR treats these reports as confidential to sponsors and does not make them available for general circulation. Individual sponsors may, however, authorize subsequent release of the material.

UNIVERSITY OF SOUTHAMPTON

INSTITUTE OF SOUND AND VIBRATION RESEARCH

DYNAMICS GROUP

An Overview of the Single Degree of Freedom System and Zener Model for Passive Shock Isolation

by

D.F. Ledezma-Ramirez, N.S. Ferguson and M.J. Brennan

ISVR Technical Memorandum No: 947

June 2005

Authorised for issue by
Professor M.J. Brennan
Group Chairman

An overview of the single degree of freedom system and Zener model for passive shock isolation.

Table of contents

Notation

c	Viscous damping constant
c_c	Critical damping
j	$\sqrt{-1}$
k	Elastic stiffness
k^*	Complex stiffness
m	Mass
t	Time
$u(t)$	Base displacement
x	Mass displacement
F	Force
I	Impulse
T	Natural period
U	Potential energy
α	Stiffness ratio in the Zener model
$\delta(t)$	Dirac delta function
ϕ	Phase angle
η	Loss factor
ν	Arbitrary transient response
τ	Rise time/pulse period
ω	Circular frequency
ξ	Arbitrary transient excitation
ζ	Viscous damping ratio
δ_x	Relative displacement
ν_m	Maximax response
ν_r	Residual response
ω_n	Natural frequency
ω_t	Transition frequency
ξ_c	Maximum step/pulse amplitude
Ω_n	Frequency ratio $\sqrt{\omega/\omega_n}$
Ω_t	Frequency ratio $\sqrt{\omega_t/\omega_n}$

Index of figures

1. -INTRODUCTION.

Transient vibration is defined as a temporarily sustained vibration of a mechanical system. It may consist of forced or free vibrations, or both [1]. Transient loading, also known as impact, or mechanical shock, is a nonperiodic excitation, which is often characterized by a sudden and severe application. In real life, mechanical shock is very common. Examples of shock could be a forging hammer, an automobile passing across a road bump, the free drop of an item from a height, etc.

For most of the cases, to analyse systems involving mechanical shock it is necessary to idealize the forcing function (displacement, velocity, acceleration or force) as a step or pulse excitation. This impulsive forcing function can be approximated to a certain shape depending on the situation and the structural characteristics of the system (natural frequency and damping ratio).

When modelling mechanical systems it is quite common to build a mathematical model of one degree of freedom representing the physical properties of the system. Normally the stiffness is represented by a linear elastic element, and damping is considered viscous, being represented by a dashpot. These elements are arranged in parallel. This approach (mass spring damper system - MKC) is relatively simple and gives very reasonable results. However, many materials have viscoelastic behaviour. A viscoelastic material is characterized by possessing both viscous and elastic behaviour. Damping is no longer due to dashpots, but it is generated by internal friction (hysteresis). Many polymeric materials such as rubber behave in this manner.

The aim of this report is to give an insight into the behaviour of the linear single degree of freedom system under shock excitation and obtaining the time and frequency response functions resulting for different impulsive forcing inputs. The effect of different pulse shapes and their duration on the response of the system is investigated. In first instance, the single mass spring system is considered, then, the effect of viscous damping will be introduced for the complete analysis of the MKC system. Then, a further analysis is performed using a more complex form of the classical system which represents the basic form of a viscoelastic material and it comprises a spring and damper in series connected in parallel to another elastic spring and is called the Zener model [5]. This model gives a good insight into the behaviour of viscoelastic materials. The analysis of this model is not only restrained to transient behaviour, since there is little published information about this system. As a result, it is interesting to look briefly at the free response of this system as well as the harmonically excited vibration. A similar analysis as that done in the MKC system is considered for pulse excitation. A comparison between the classical MKC model and the Zener model is made describing the advantages and disadvantages of each one.

2. - DEFINITIONS

To avoid confusion, it is necessary to introduce and define some useful terminology which will be used through this report.

A spectrum is a plot of the response, chosen to represent one aspect of the effect of the forcing function on the system, against the ratio of the characteristic period or frequency of the forcing function to the natural period or frequency of the system [2]. Regarding shock phenomena, it is more convenient to use the period (duration) of the impulse, and the natural period of the system involved, rather than frequencies. This approach is convenient because for transient loading the excitation is relatively short in duration, or has the nature of a single pulse. This leads to the use of a period spectrum [2].

The maximum absolute displacement, velocity, or acceleration of the system occurring at any time as a result of the forcing function, is called the *maximax response* , denoted by v_m [2].

The maximum displacement of the system during the residual vibration phase after the loading has been removed is called the residual amplitude, and measured with respect to the final position of equilibrium, denoted by v_r [2]. In some cases, $v_r = v_m$, but this is not the general case which is $v_r \leq v_m$.

3. - SINGLE DEGREE OF FREEDOM, UNDAMPED SYSTEMS

3.1. - Equation of motion.

Consider a linear single degree of freedom system, with no damping as shown in figure 3.1. It comprises a mass supported on an elastic stiffness, the latter representing an undamped isolator. The input is a function of time, and may be a force acting on the mass, or a displacement of the base or foundation. Sometimes it is more convenient to express it as ground acceleration. (Fig. 3.1.c)

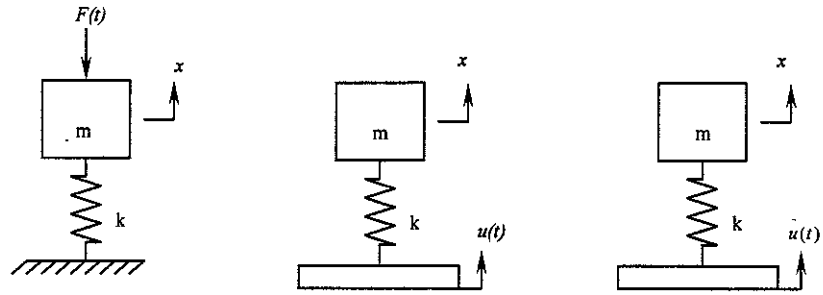

(a) (b) (c)

Figure. 3.1. - Single spring-mass system, subjected to impulsive excitations. (a) Force $F(t)$, (b) Ground displacement $u(t)$, (c) Ground acceleration $\ddot{u}(t)$.

The differential equations governing the motion of the systems shown in figure 3.1 are:

Figure 1(a)

$$m\ddot{x} = -kx + F(t) \qquad \text{or} \qquad \frac{m\ddot{x}}{k} + x = \frac{F(t)}{k} \tag{3.1}$$

Figure 1(b)

$$m\ddot{x} = -k\left[x - u(t)\right] \qquad \text{or} \qquad \frac{m\ddot{x}}{k} + x = u(t) \tag{3.2}$$

Figure 1(c)

$$m\left[\ddot{\delta}_x + \ddot{x}(t)\right] = -k\delta_x \qquad \text{or} \qquad \frac{m\ddot{\delta}_x}{k} + \delta_x = \frac{-m\ddot{u}(t)}{k} \tag{3.3}$$

Where x is the absolute displacement of the mass relative to a fixed reference, and δ_x is the displacement relative to a moving ground. The relationship between these displacements and the ground displacement is $x = u + \delta_x$.

In this report, the motion of a system is described using a more general form of the equations (3.1 - 3.3). The equation is:

$$\frac{\ddot{v}}{\omega_n^2} + v = \xi(t) \tag{3.4}$$

Where ω_n is the natural frequency of the system and it is equal to $\sqrt{k/m}$, v is the response of the system, and ξ the excitation, both functions of time. However, sometimes it is necessary to express the excitation and response using a more specific notation. Alternative forms of excitation and response are given in table 1[1].

Excitation $\xi(t)$		**Response** $v(t)$	
Force	$F(t)$	Absolute displacement	x
Ground displacement	$u(t)$	Absolute displacement	x
Ground acceleration	$\ddot{u}(t)$	Relative displacement	δ_x
Ground acceleration	$\ddot{u}(t)$	Absolute acceleration	$\ddot{x}$
Ground velocity	$\dot{u}(t)$	Absolute velocity	$\dot{x}$
nth derivative of the ground displacement	$\frac{d^n u}{dt^n}(t)$	nth derivative of absolute displacement	$\frac{d^n x}{dt^n}$

Table 3.1. - Alternative forms of the excitation and response of equation (3.4).

3.2. - Step-like and pulse-like excitation.

Impulsive excitation produces vibrational responses in elastic systems, and the maximum values of these responses may be less than, equal to, or greater than the corresponding static response [3]. In general, the response depends upon the system properties and the nature of the load. For single degree of freedom systems a characteristic that determines the response is the natural period (or natural frequency). In addition, the shape and duration of the impulse plays an important role in the response. Shock phenomena can be modelled using ideal step and pulse functions, which represent very well the features of real transient inputs and which also produce similar system behaviour. However, when the duration of the shock is very short in comparison with the natural period, it can be simply represented by a scaled version of the unit impulse. The following analysis is based on the assumption that the system is initially at rest.

3.2.1. - The unit impulse.

Many situations involving shock excitation can be considered as the result of applying a unitary impulse to the system, as long as the period of the shock tends to zero (a sharp pulse). This sort of transient excitation can be treated

mathematically using the Dirac delta function $\delta(t)$. The Dirac delta function can be defined as:

$$\delta(t) = 0 \qquad t \neq 0 \tag{3.5}$$

and

$$\int_{-\infty}^{\infty} \delta(t)dt = 1 \tag{3.6}$$

Figure 3.2 shows the graphical representation of the Dirac delta function. Its representation is a single impulse of area equal to unity at $t=a$.

When a sudden impulse I is applied to an undamped single degree of freedom system at rest, it can be shown that the subsequent response is given by [6]:

$$x(t) = \frac{I}{m\omega_n} \sin(\omega_n t) \tag{3.7}$$

Where $x(0) = 0$ and $\dot{x}(0) = I/m$.

This is represented graphically in figure 3.3. It is noticeable that the maximax response occurs after the impulse has been applied. If I is of unit magnitude then the response is the impulse response function given by eq. 3.7.

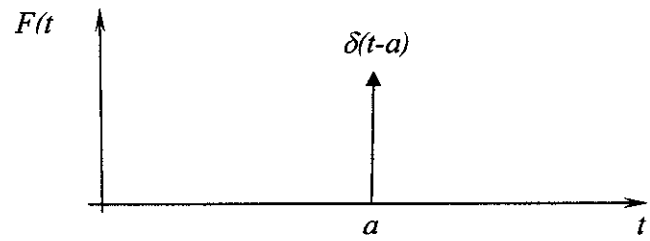

Figure 3.2. - Representation of the Dirac delta function

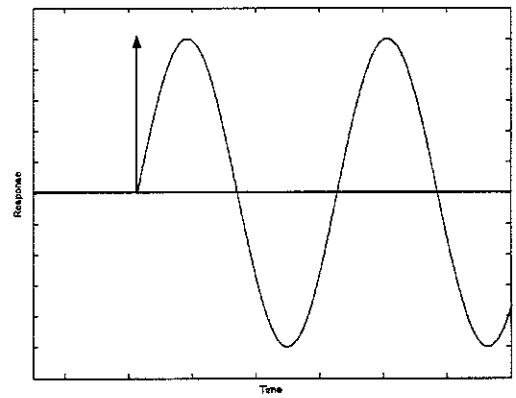

Figure 3.3. - Response of an undamped single degree of freedom system to a unit impulse

3.2.2. - Step type excitation functions.

The most fundamental transient excitation is the form of the step function. To be fully realistic these functions must describe the translation of the system through a finite distance, in a finite time, with finite acceleration and deceleration [4]. Many functions rise to their maximum constant value ξ_c in a finite time τ, called the *rise time*. Consider the following base excitation functions and the expressions for the maximax response given in [1]:

a) Constant slope front.

$$\xi(t)=\begin{Bmatrix}\xi_c\dfrac{t}{\tau} & [0\le t\le\tau]\\ \xi_c & [\tau\le t]\end{Bmatrix} \tag{3.8}$$

$$\frac{\nu_m}{\xi_c}=1+\left|\frac{T}{\pi\tau}\sin\left(\frac{\pi\tau}{T}\right)\right| \tag{3.9}$$

b) Versed sine front.

$$\xi(t)=\begin{Bmatrix}\dfrac{\xi_c}{2}\left(1\text{-}\cos\left(\dfrac{\pi t}{\tau}\right)\right) & [0\le t\le\tau]\\ \xi_c & [\tau\le t]\end{Bmatrix} \tag{3.10}$$

$$\frac{\nu_m}{\xi_c}=1+\left|\frac{1}{\left(4\tau^2/T^2\right)-1}\cos\left(\frac{\pi\tau}{T}\right)\right| \tag{3.11}$$

c) Cycloidal front.

$$\xi(t)=\begin{Bmatrix}\dfrac{\xi_c}{2}\left(\dfrac{2\pi t}{\tau}\text{-}\sin\left(\dfrac{2\pi t}{\tau}\right)\right) & [0\le t\le\tau]\\ \xi_c & [\tau\le t]\end{Bmatrix} \tag{3.12}$$

$$\frac{\nu_m}{\xi_c}=1+\left|\frac{1}{\pi\tau\left(1-\tau^2/T^2\right)}\sin\left(\frac{\pi\tau}{T}\right)\right| \tag{3.13}$$

Where T is the natural period of the single degree of freedom system involved. The plots for the excitation function and the time response curves are superimposed in fig. 3.4. They were calculated using Laplace

transformations of equation 3.4 for the different inputs and algebraic manipulation using MAPLE to obtain the symbolic expressions for the time response. The process of obtaining the response using Laplace transformations is given in appendix 1 for several of the cases considered here.

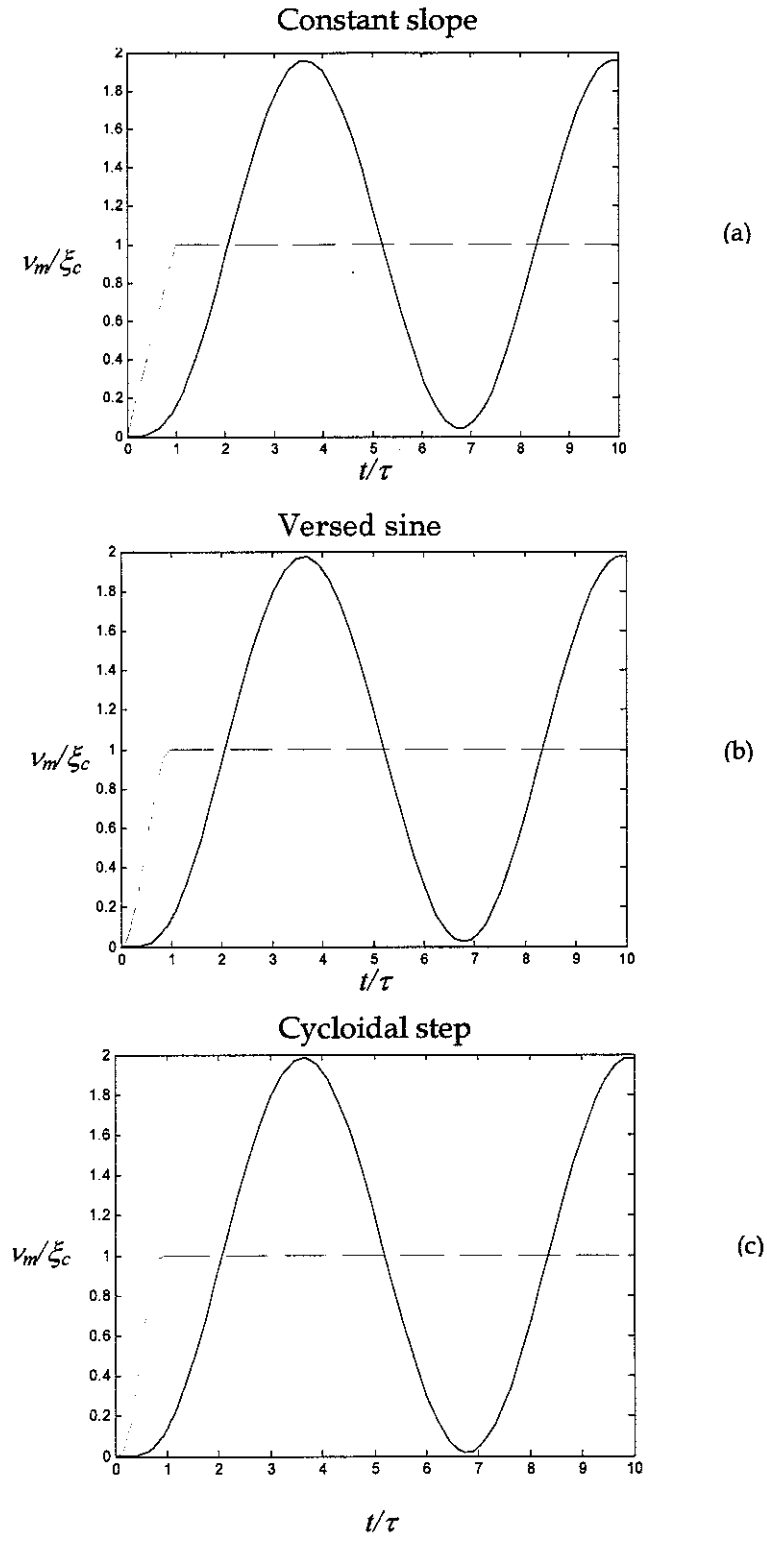

Figure 3.4 .- Displacement response curves and excitation functions for (a) constant slope step, (b) versed sine step, (c) cycloidal step. [——— System response] [- - - - - Excitation]

3.2.3 Symmetrical pulses.

A pulse-like excitation is a more complex function. It can be considered as being equivalent to the superposition of two or more successive input functions. For example, a half sine pulse can be obtained by the addition of two sine inputs with one delayed by half the sinusoid period. Consider three single symmetrical pulses: rectangular, half sine and versed sine. The excitation functions $\xi(t)$ and time response v equations are given by the following equations [1]. Residual response factors are also given and correspond to the solutions for $[\tau \le t]$.

a) Rectangular

$$\left\{\begin{aligned}\xi(t) &= \xi_c \\ v &= \xi_c\left(1-\cos\left(\omega_n t\right)\right)\end{aligned}\right\} \qquad [0 \le t \le \tau] \qquad (3.14)$$

$$\left\{\begin{aligned}\xi(t) &= 0 \\ v &= \xi_c\left[2\sin\left(\frac{\pi\tau}{T}\right)\right]\sin\omega_n\left(t-\frac{\tau}{2}\right)\end{aligned}\right\} \qquad [\tau \le t] \qquad (3.15)$$

b) Half cycle sine

$$\left\{\begin{aligned}\xi(t) &= \xi_c \sin\left(\frac{\pi t}{\tau}\right) \\ v &= \frac{\xi_c}{1-T^2/4\tau^2}\left(\sin\left(\frac{\pi\tau}{\tau}\right)-\frac{T}{2\tau}\sin\omega_n t\right)\end{aligned}\right\} \qquad [0 \le t \le \tau] \qquad (3.16)$$

$$\left\{\begin{aligned}\xi(t) &= 0 \\ v &= \xi_c\left[\frac{(T/\tau)\cos(\pi\tau/T)}{\left(T^2/4\tau^2\right)-1}\right]\sin\omega_n\left(t-\frac{\tau}{2}\right)\end{aligned}\right\} \qquad [\tau \le t] \qquad (3.17)$$

c) Versed sine

$$\left\{\begin{aligned}\xi(t) &= \frac{\xi_c}{2}\left(1-\cos\left(\frac{2\pi t}{\tau}\right)\right) \\ v &= \frac{\xi_c/2}{1-\tau^2/T^2}\left(1-\frac{\tau^2}{T^2}+\frac{\tau^2}{T^2}\cos\left(\frac{2\pi t}{\tau}\right)-\cos\left(\omega_n t\right)\right)\end{aligned}\right\} \qquad [0 \le t \le \tau] \qquad (3.18)$$

$$\left\{\begin{aligned}\xi(t) &= 0 \\ v &= \xi_c\left[\frac{\sin(\pi\tau/T)}{1-\tau^2/T^2}\right]\sin\omega_n\left(t-\frac{\tau}{2}\right)\end{aligned}\right\} \qquad [\tau \le t] \qquad (3.19)$$

The response curves and excitation as functions of time are shown in fig. 3.5, for different values of the ratio τ/T which is the duration of the input compared to the period of the SDOF system. The solutions of the equations of motion were obtained using Laplace transformations for the various cases. When the impulse is very short ($\tau/T < 0.25$) the pulse tends to approach the Dirac delta function, and the response can be approximated using the simple unit impulse theory. As a result, the shape of the pulse is of negligible importance. On the other hand, when the period of the impulse is very long compared to the natural period ($\tau/T > 2$), the response follows the shape of the impulse closely during the time when the input is applied. In all of the input types considered here, for certain values of τ/T there is no residual response. This fact can be proved considering that the total work done by the excitation force is equal to zero. For a complete proof see appendix 2.

3.3. - Shock spectrum.

Any general mechanical system is capable of transient vibrations, and also there is the potential for resonances at a number of frequencies [5]. The primary effect of shock is to excite mounted mechanical or electrical equipment and to cause it to respond in its modes of vibration. As a result, damage or malfunction may take place. Typically, the subsequent vibration decays depending on the amount of damping present in the system. The peak acceleration and peak relative displacement of the system are particularly important as these often indicate whether damage or failure may occur.

A spectrum is defined as a plot of a response quantity (displacement, velocity or acceleration), against the ratio of the period or frequency of the forcing function, to the natural period or frequency of the system. In this report the term shock response spectra is used, but it can also be regarded simply as response spectra. A shock spectrum is simply the peak acceleration or displacement produced by the shock on the isolated mass as a function of the natural frequency of the mass on its elastic support [4]. Shock spectra can be measured experimentally, computed from waveforms, or determined theoretically. Such diagrams are of interest in design, because they provide the possibility of predicting the maximum dynamic stress [3] and potential damage in the system.

In fact, the shock spectrum gives a full and realistic measure of the damaging potential of a shock disturbance. To select a damage criterion (acceleration or displacement), the duration of the pulse and the natural period of the system are of great importance (considering a SDOF undamped system). If, $T << \tau$ the motion of the mass closely follows the motion of the support during the shock input (see figure 3.5 for values of τ/T greater than 2). The acceleration then becomes the primary quantity of concern. Otherwise, when $T >> \tau$, the mass remains substantially at rest until motion of the support has ceased (as

shown in figure 3.5 for values of τ/T less than 0.5), and it is the value of the maximum displacement that determines potential damage. Moreover, if the transient disturbance is neither short nor long duration to fit into one of the previous cases, no simple damage criterion can be found [4]. As a result both acceleration and displacement must be considered.

Ratio τ/T	Rectangular	Half sine	Versed sine
1/4	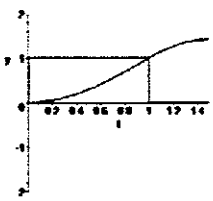	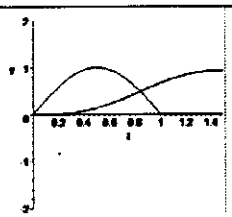	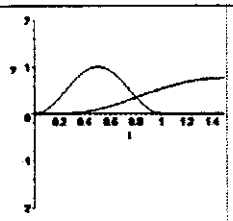
1/2	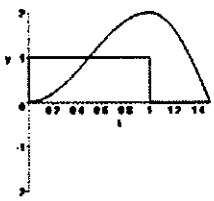	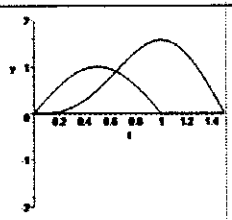	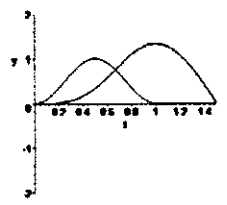
1	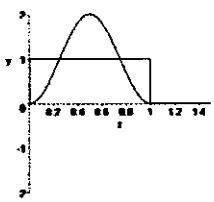	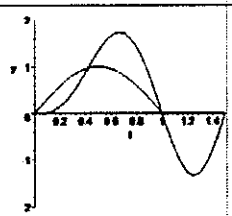	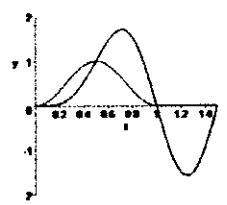
3/2	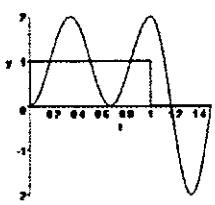	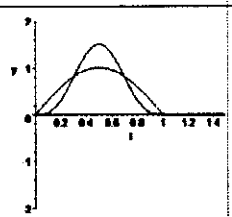	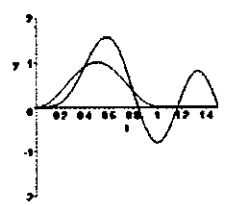
2	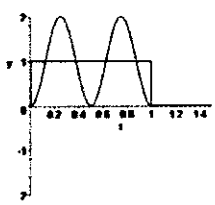	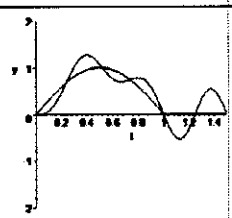	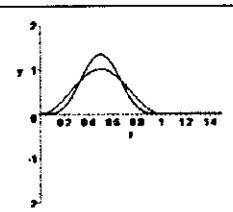
5/2	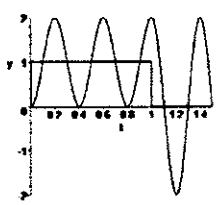	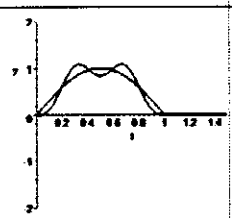	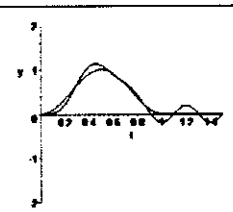

Figure 3.5.- Displacement response curves for several symmetrical pulses; rectangular, half sine, and versed sine, for different values of τ/T

3.3.1 - Shock spectra for particular pulse and step shapes.

Further insight into the significance of shock spectra can be obtained by studying the spectra corresponding to a number of simple shapes [5]. Fig. 3.6 shows the spectra for the maximax response resulting from the step functions discussed in section 3.1.2, plotted as a function of the ratio between the rise time and natural period of the system. The maximax response for the step functions (equations 3.9, 3.11 and 3.13) occurs after the excitation has reached its constant maximum, and is related to the residual amplitude by [1]:

$$\nu_m = \nu_r + \xi_c \tag{3.20}$$

Where ξ_c is the maximum constant value reached by the step function, and it is given by F/k if the excitation is a force applied to the mass, or by $u(t)$ if it is a ground motion.

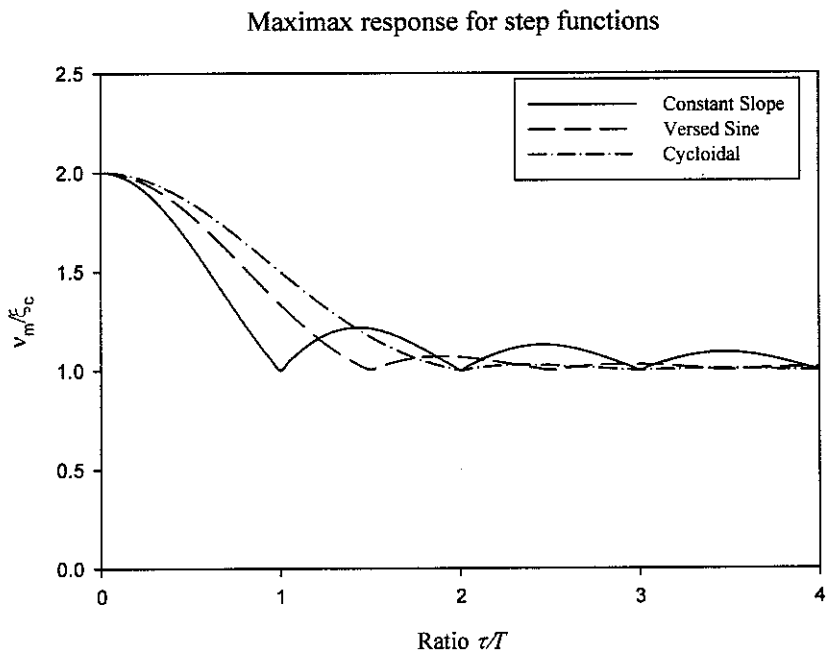

Figure 3.6. - Shock response spectrum for three step functions; constant slope, versed sine and cycloidal .

By examining figure 3.6 one can observe that the extreme values of the ratio of maximum response to step height ν_m/ξ_c are 1 and 2. When the ratio of step rise time to natural period τ/T tends to 0 (a very short rise time compared to the natural period), ν_m/ξ_c tends to its maximum of 2, and when τ/T approaches infinity, the step is no longer a dynamic excitation but it is quasi static, in consequence the inertia forces of the system tends to zero, and ν_m/ξ_c approaches the lower value of 1 [1].

It is clear that for certain values of τ/T, the ratio ν_m/ξ_c is equal to 1. The lowest value of τ/T for which $\nu_m/\xi_c = 1$ are for a constant slope input, $\tau/T = 1.0$, versed sine input, $\tau/T = 1.5$ and cycloidal input, $\tau/T = 2.0$ [1].

Response spectra for symmetrical pulses (rectangular, half-sine and versed sine) are shown in fig. 3.7. A further analysis of these plots and the time response curves (Fig. 5) reveals that for values of τ/T less than 0.25 (corresponding to short duration pulses), the shape of the pulse is of less importance in determining the maximum value of the response. This behaviour can be explained by considering that the response is essentially due to an impulse, because the pulse has a very short duration. In contrast, if τ/T is larger than 0.5, the shape may be of greater significance. The response tends to become quasi static and it follows closely the shape of the input. It is clearly seen that isolation (ν_m/ξ_c being less than 1) can be possible only in a very low range of values of τ/T, approximately less than 0.27 for the half sine pulse and similar values for the other forcing functions. This means low natural frequency mounts.

The maximum value of the residual response amplitude for the input types discussed is often a good approximation to the maximum of maximax response, and they occur at values of τ/T not greatly different from each other [1].

In general, the residual response amplitude generally has zero values for certain finite values of τ/T [1]. This fact can be proved considering that the total work done by the forcing function is equal to zero. A complete proof is given in appendix 2.

Another parameter of great importance apart from maximax absolute response and residual response is the maximax relative response, which represents the deformation in the elastic element, in the case of base displacement excitation. This parameter is useful to obtain the stresses in the elastic element due to the excitation, and is defined as: $x = u + \delta_x$ (Refer to figure 3.1), and it can occur during the excitation period or in the residual vibration, in this case being equivalent to the residual response [1].

So far, the excitation $\xi(t)$ and the response $\nu(t)$ considered can take any of the forms considered in table 1. Nevertheless, it is worth to look at a particular case and investigate the nature of the response and its derivatives for a certain excitation. Take for example the case of base displacement as an excitation. The displacement response has already been analyzed in figure 3.7 for the several forcing functions considered. But for certain applications the quantity of concern is the acceleration, rather than the displacement. Figure 3.8 shows the shock response spectra for maximax acceleration due to a base

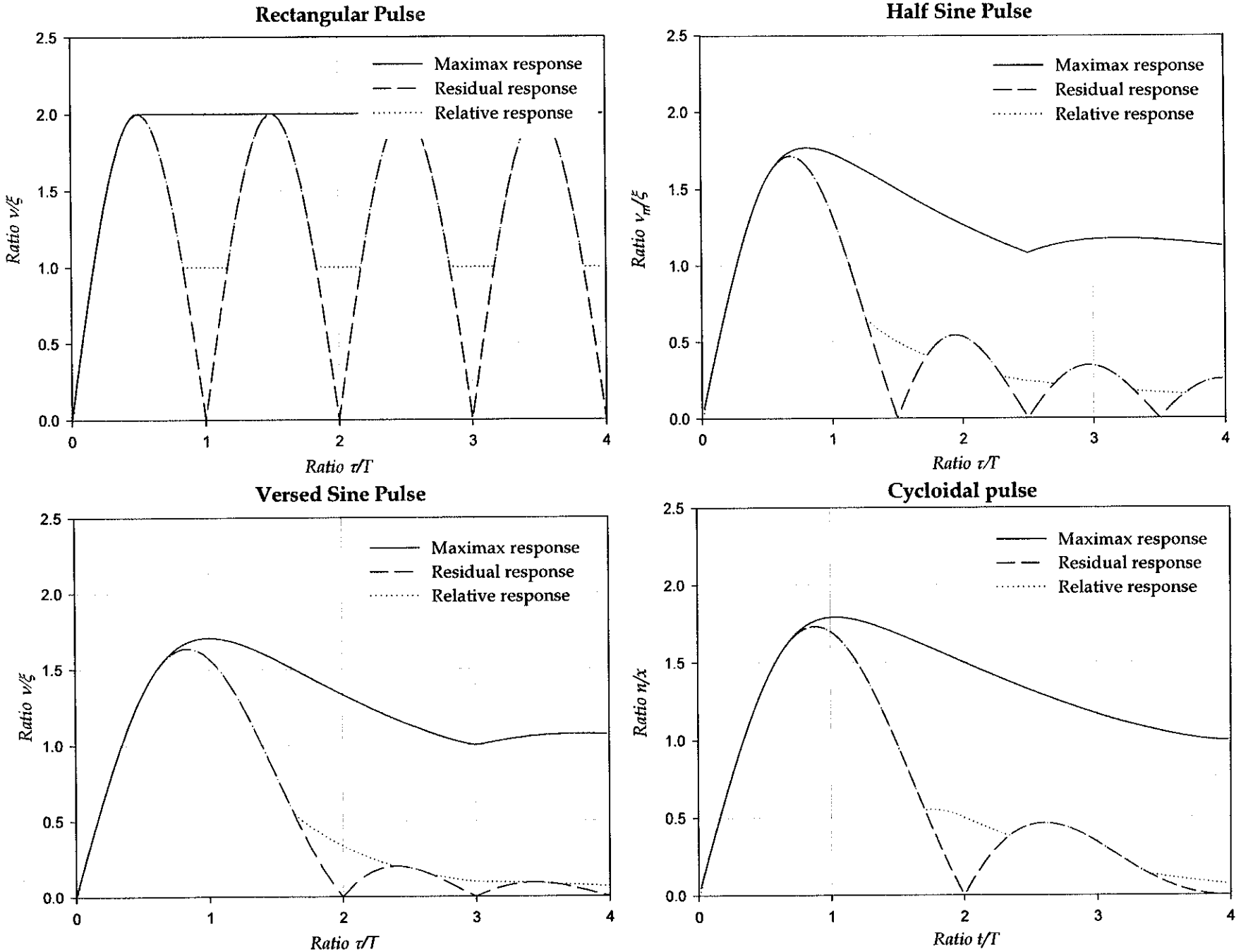

Figure 3.7 . – Response spectra showing maximax and residual response, for an undamped single degree of freedom system with natural period T, and τ being the period of the shock, for (a) rectangular, (b) half sine, (c) versed sine, (d) cycloidal

displacement shock excitation for half sine and versed sine pulses. A comparison with figure 3.7 reveals that for $\tau/T \leq 0.5$ the acceleration is not as significant as the displacement, but for higher values of τ/T the acceleration becomes of great importance. Similar results are observed for both half sine and versed sine, although the latter case shows lower overall values.

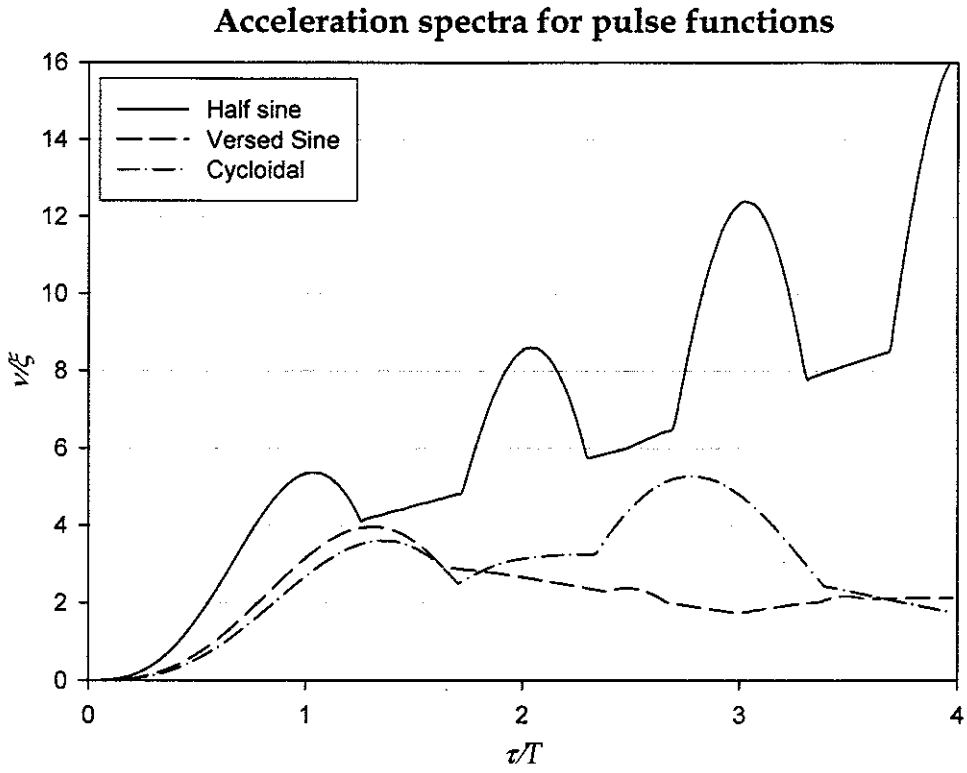

Figure 3.8. - Response spectra showing maximax acceleration response for an undamped single degree of freedom system with natural period T, and τ being the period of the shock, half sine pulse, versed sine pulse.

4. -SINGLE DEGREE OF FREEDOM, VISCOUSLY DAMPED SYSTEMS

For steady forced vibration, even if the system has low damping, damping is of great importance in limiting the response near resonance. However, if the excitation is a pulse or step function, the effect of damping may be of less importance, unless the system is highly damped [1]. Nevertheless, as a result of the introduction of damping in the system, the maximax response as well the residual response may decrease. Generally, less work had been reported on the effect of damping on systems undergoing shock excitations.

For a viscously damped system, the equation of motion under general notation, is:

$$\frac{m}{k}\ddot{v}+\frac{c}{k}\dot{v}+v=\xi(t) \tag{4.1}$$

or

$$\frac{1}{\omega_n^2}\ddot{v}+\frac{2\zeta}{\omega_n}\dot{v}+v=\xi(t) \tag{4.2}$$

Where c is the viscous damping constant and ζ is the damping ratio of the system.

Figure 4.1 shows the maximax response spectrum for a single degree of freedom system with viscous damping, subjected to a half sine pulse excitation as a function of the viscous damping ratio. Comparing figure 4.1 with figure 3.7 one can observe that in all cases there is a benefit of having damping present [1]. Progressively increasing the amount of damping results in a decrease in the maximax response for $\tau/T<2$. However, when τ/T takes very large values the excitation becomes quasi static and the normalized response always tend to 1 and damping has no further effect.

In general, increasing damping levels will reduce the residual response as well. The behaviour of the system once the shock has finished is essentially free vibration. As a result, damping values above the critical value will result in longer times to get back to the equilibrium position.

Further insight into the behaviour of damped systems under shock excitation can be obtained from figure 4.2, which is a plot of the ratio of the maximum value of the shock response spectra for a damped system to the undamped system, for various values of damping. This plot has been done considering the maximum value of the maximax response for every forcing function considered (τ/T =0.5 for rectangular pulse, τ/T =0.8 for half sine pulse and τ/T =1 for versed sine pulse), and other values of τ/T. It is clear that the effect

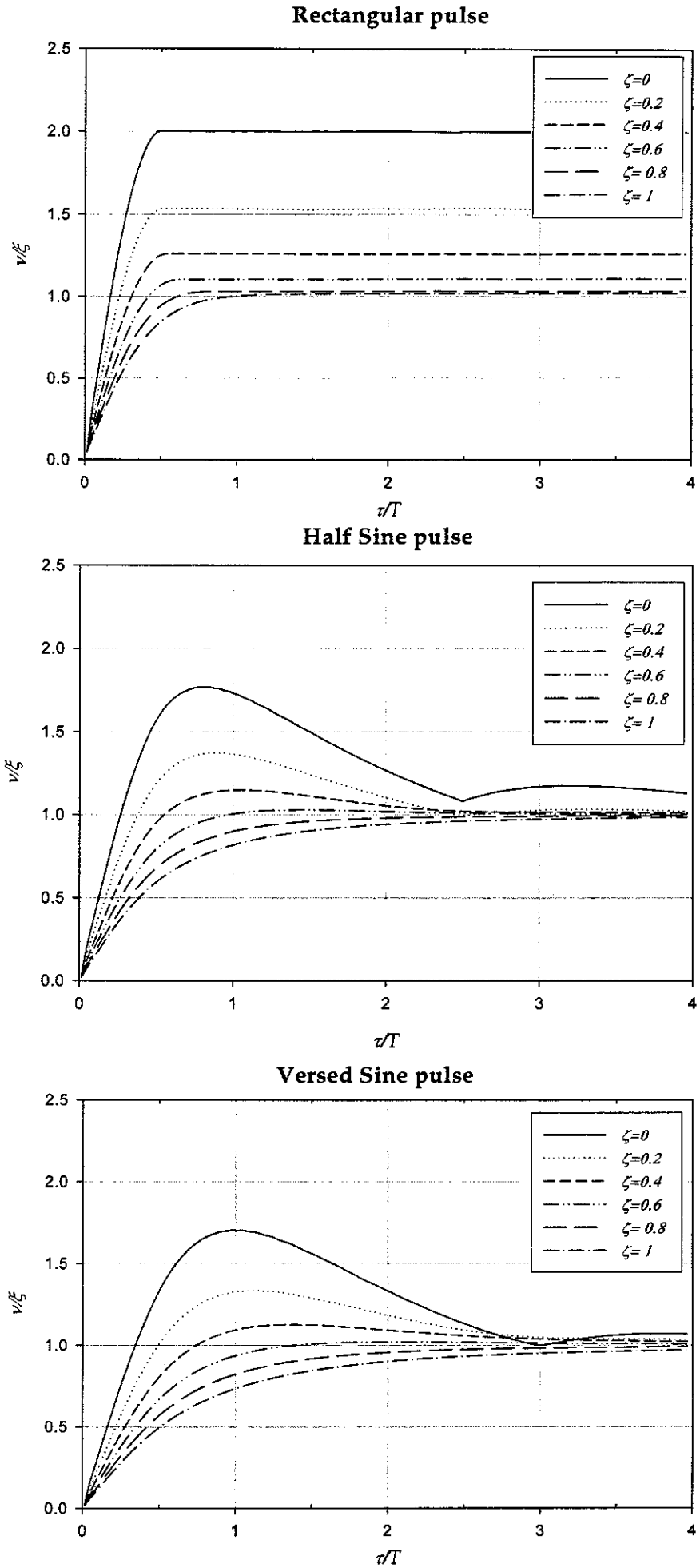

Figure 4.1.- Maximax response spectrum for a single degree of freedom system with viscous damping for (a) rectangular pulse, (b) versed sine pulse, (c) half sine pulse, for various values of damping ratio.

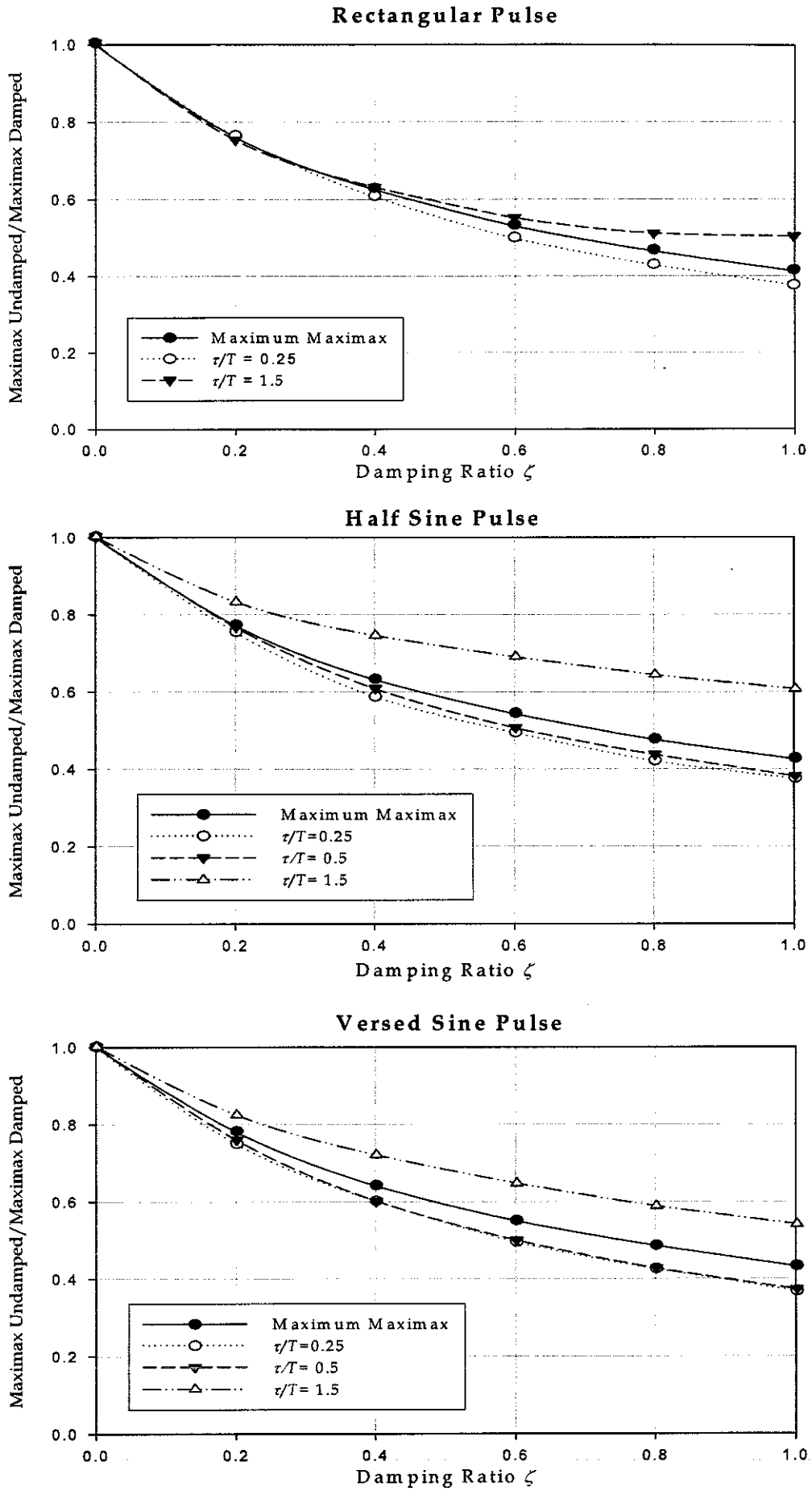

Figure 4.2. - Effect of damping in the reduction of maximax response for three different inputs: (a) Rectangular, (b) Half sine, (c) Versed sine. Vertical axis represents the ratio between the maximax for a damped system and the maximax for an undamped system. Horizontal axis is the value of damping ratio.

of damping is similar for the three transient excitation inputs considered, and is also similar for the different values of τ/T considered. Large reductions in the response can be achieved for larger values of damping, but care has to be taken because of the derivatives of the response can take higher values as damping increase, as explained below. Another result of damping values higher than the critical value is a longer time to get back to the initial position.

On the other hand, considering the forcing function as a base displacement and the response as an acceleration in the mass, the acceleration spectra are shown in figure 4.3. As mentioned before, for $\tau/T \leq 0.5$ the displacement is the quantity of concern rather than the acceleration. Moreover, when damping is present, it has almost no effect in this range of values of τ/T but its effect becomes important for higher values of τ/T. A decrease of acceleration is observed for low values of damping ratio $0.2 \leq \zeta \leq 0.3$ but higher values of damping will end up with large accelerations levels, especially when τ/T is large. Mindlin [17] has effectively predicted this behaviour for package design using free drop tests. The shock response spectra presented here for the two forcing functions considered clearly show the described behaviour. Moreover, similar results are observed for both forcing functions. Nonetheless, the versed sine case presents lower acceleration levels than the half sine pulse. As a result, it can be said that the half sine pulse can be regarded as a worst case scenario. In fact, the half sine pulse is widely used in shock testing [5,17,18]. The effect of damping on the acceleration can be fully appreciated in figure 4.4 for different values of τ/T, in which the ratio between the maximax acceleration for the undamped system and the damped system is shown as a function of damping ratio.

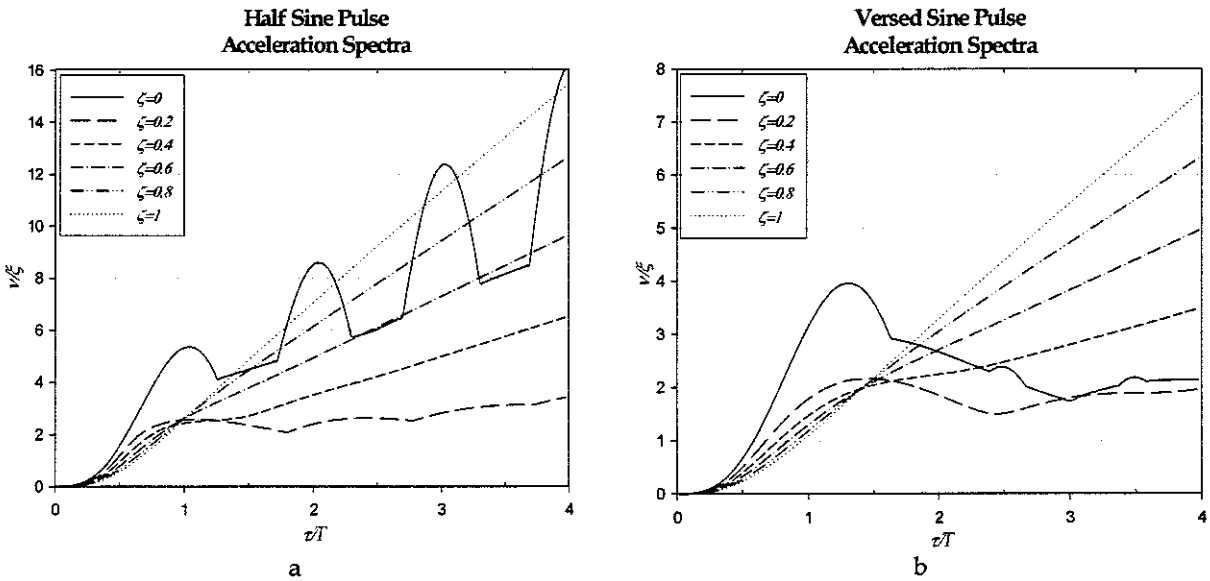

Figure 4.3- Maximax response spectrum for acceleration of a single degree of freedom system with viscous damping (a) half sine pulse, (b) versed sine pulse, for various values of damping ratio.

5. - INTERNAL DAMPING.

The form of damping considered in the previous section was viscous. This concept is physically and mathematically simple. It allows good solutions to be obtained in a straightforward manner without mathematical complexities. However in practice, different damping mechanisms exist and they are not as simple as the viscous one.

Viscous damping is an external mechanism which dissipates energy. Another external way to dissipate energy is dry friction, or Coulomb damping. Nevertheless, there are internal mechanisms of damping. In a wider sense internal damping is also called *structural or material damping*.

All real materials dissipate some energy during cyclic load, due to structural damping. Polymeric materials, in special rubber, exhibit a high amount of energy dissipated [9]. Another important characteristic of these materials is that they not only present a high amount of damping, but also behave in an elastic manner. This characteristic is called *viscoelasticity*. A further understanding of the behaviour and properties of viscolelastic materials is necessary because they are widely used as anti vibration mounts.

5.3. - Models used to represent viscoelasticity.

Several models have been developed to represent mechanical systems using viscous damping and elastic elements. The classical approach is the configuration shown in figure 5.1(b). It includes a dashpot in parallel with an elastic spring. This system is also called the Kelvin model. This model is quite simple, but poorly represents the characteristics of a viscoelastic material. This system has been improved adding a spring in series with the dashpot and the result is the so-called Zener model, shown in figure 5.1(c). Further enhancements can be done by adding more elements as shown in figure 5.1(d), increasing the complexity of the system, but also increasing the accuracy of the results in representing the complex frequency domain behaviour of a viscoelastic material.

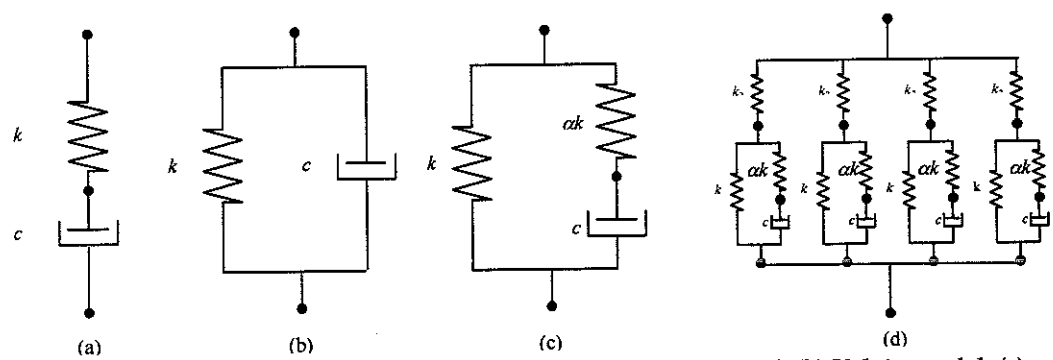

Figure 5.1. - Models of viscolelastic behaviour. (a) Maxwell model, (b) Kelvin model, (c) Zener model, (d) A more complex idealization of a viscoelastic material.

6. - DYNAMIC DAMPING AND STIFNESS IN THE ZENER MODEL.

6.1. - Relaxation

The Zener model [11] is also called *viscous-relaxation* system. In general the Zener model is the simplest representation of a viscoelastic material. Some particular phenomena in viscoelastic materials are [12]:

- Creep: if the stress is held constant, the strain increases with time.
- Relaxation: if the strain is held constant, the stress decreases with time.
- The effective stiffness depends on the rate of application of the load.
- When cyclic load is applied, hysteresis occurs, leading to a dissipation of mechanical energy.

Generally the physical properties of viscoelastic materials are influenced by many factors, like temperature, frequency, dynamic strain rate, static pre-load, aging, etc, depending on the damping mechanism. In this system, the phenomenon of relaxation is the principal damping mechanism. One of the principal characteristic of the relaxation is that both the overall stiffness and loss factor are highly frequency dependant (see appendix C).

7. - FREE VIBRATION OF THE ZENER MODEL.

7.1 Derivation of equation of motion

In order to investigate the response of a Zener model subject to free oscillations, it is necessary to derive the equation of motion. Consider the system in figure 7.1. When the mass m is displaced a distance x, it moves around its equilibrium position, while the junction point between the dashpot c and the spring αk experiences a displacement x_0.

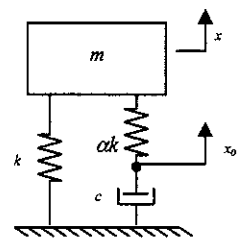

Figure 7.1. - Zener model for free vibrations. Distance x is the absolute displacement of the mass m from its equilibrium position and x_0 represents the displacement of the connection of the dashpot c to the spring αk.

The equation of motion for the mass from Newton's laws of motion is:

$$m\ddot{x} + kx + \alpha k\left(x - x_0\right) = 0 \tag{7.1}$$

Since the dashpot c and the spring αk are arranged in series, and applying force equilibrium at the connection point, one can write:

$$c\dot{x}_0 + \alpha k(x - x_0) = 0 \tag{7.2}$$

To obtain a single equation in terms of the mass displacement x, equation 7.1 is differentiated once with respect to time:

$$m\ddot{x} + k\dot{x} + \alpha k\dot{x} - \alpha k\dot{x}_0 = 0 \tag{7.3}$$

After algebraic manipulation of equations 7.1 and 7.2, it is evident that:

$$\dot{x}_0 = -\left(\frac{m\ddot{x} + kx}{c}\right) \tag{7.4}$$

Rearranging equations 7.3 and 7.4, one can obtain the third order differential equation of motion of the Zener system:

$$m\dddot{x} + \frac{\alpha km}{c}\ddot{x} + k(\alpha + 1)\dot{x} + \frac{\alpha k^2}{c}x = 0 \tag{7.5}$$

Finally, dividing equation 7.5 by m, and considering the definition of damping ratio $\zeta = c/c_c$ where $c_c = 2m\omega_n$, and natural frequency $\omega_n = \sqrt{k/m}$ one obtains:

$$\dddot{x} + \frac{\alpha\omega_n}{2\zeta}\ddot{x} + \omega_n^2(\alpha + 1)\dot{x} + \frac{\alpha\omega_n^3}{2\zeta}x = 0 \tag{7.6}$$

7.2 Analysis of the free response

7.2.1. - Root locus analysis of the Zener model.

When investigating the free response of mechanical systems a very useful tool is the *root locus* diagram. This plot shows the path followed by the roots of the characteristic equation of a system when a particular parameter is varied from very small to very large values. The roots are plotted in the *complex plane*, or *s-plane*. When the roots are plotted in this way, inspection of the plot reveals the nature of the free response of the system. A summary of the interpretation of this plot for the single degree of freedom MKC system is given in appendix D.

This approach is used to investigate the free response of the Zener system. From section 7.1, the differential equation of motion of the Zener system is given by equation 7.6 with the resulting characteristic equation given by:

$$s^3 + \frac{\alpha\omega_n}{2\zeta}s^2 + \omega_n^2(\alpha + 1)s + \frac{\alpha\omega_n^3}{2\zeta} = 0 \tag{7.8}$$

The general solution of this equation can be written as:

$$x(t) = Ae^{s_1 t} + Be^{s_2 t} + Ce^{s_3 t} \tag{7.9}$$

Where s_1, s_2, s_3 are the roots of equation 7.8 and A, B, C are arbitrary constants that depend on the initial conditions. It is quite complicated to obtain analytical expressions for the roots. In this work the roots have been calculated numerically using MATLAB. Figure 7.3 show the root locus diagrams for α=1, 5, 8 and 15. These plots have been obtained varying the damping ratio in the characteristic equation in order to obtain the roots. Note that the path followed by the roots has been indicated with arrows, and the three roots are marked with different symbols.

From the analysis of these plots several observations can be made. Since in this case the characteristic equation has three roots, the free response depends on the nature and magnitude of these roots and the arbitrary constants A, B and C. Several situations can occur depending on the value of these roots. The total response is the sum of the response of a second order system given by the two complex conjugate roots which represents the oscillatory behaviour of the system, and the exponential solution given by the value of the real root.

For a comprehensive analysis of the free response, time displacement curves are presented in figure 7.4, where the displacement has been normalized by the initial displacement x_0. In general, for any value of α when the damping ratio is very small the value of the root s_1 is negative and very large in magnitude (graphically it is further to the left) while the other roots are complex conjugates located very near to the imaginary axis. This causes the behaviour shown in figure 9 where an oscillatory underdamped behaviour is observed for values of damping less than 0.5. As long as the damping ratio increases, the amplitude of oscillation decreases. Regarding the root locus diagram, this can be explained because now the roots s_2 and s_3 are complex conjugates and s_1 becomes larger. On the other hand, when $\alpha \geq 8$ there is a point where all the roots are real, (the system becomes critically damped). This point depends on the value of α but commonly this behaviour occurs for small values of damping ratio (less than 1). Again when the damping ratio increases, the amplitude of oscillation decays, and the system experiences an overdamped behaviour. It is important to note that the extreme cases $\alpha \approx 0$ and $\alpha \approx \infty$ are not included here, but they represent approximately the behaviour of the single undamped mass spring system and the mass spring damper system respectively.

In general, it can be said that the properties of the Zener are dependant of the value of α. The importance of this characteristic resides in the fact that damping properties could be properly tuned by adjusting basically the value of α. This indicates an advantage over the classical system.

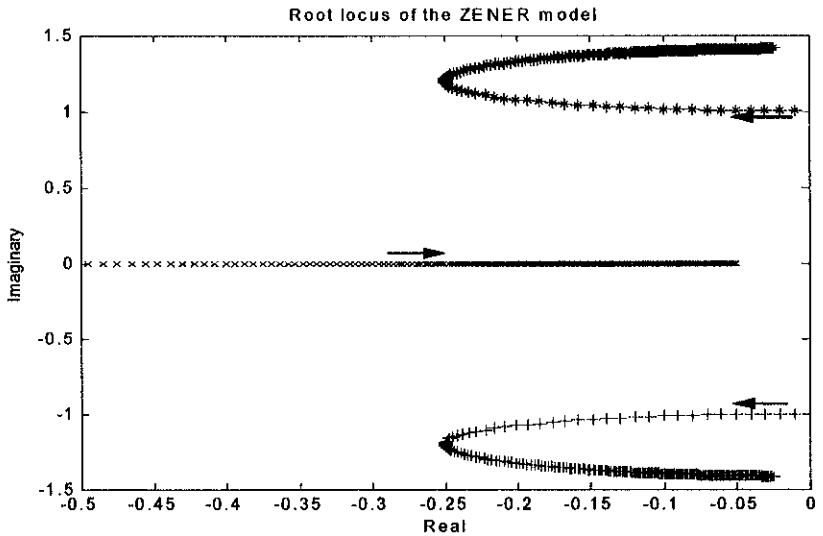

(a)

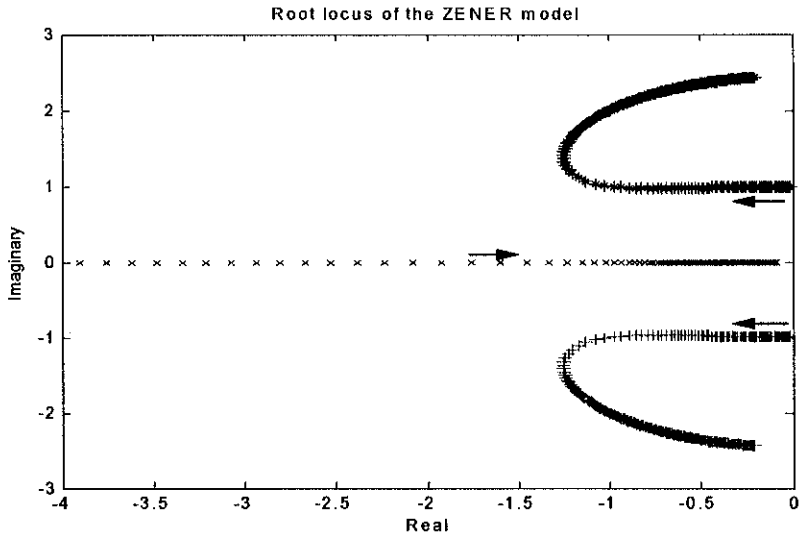

(b)

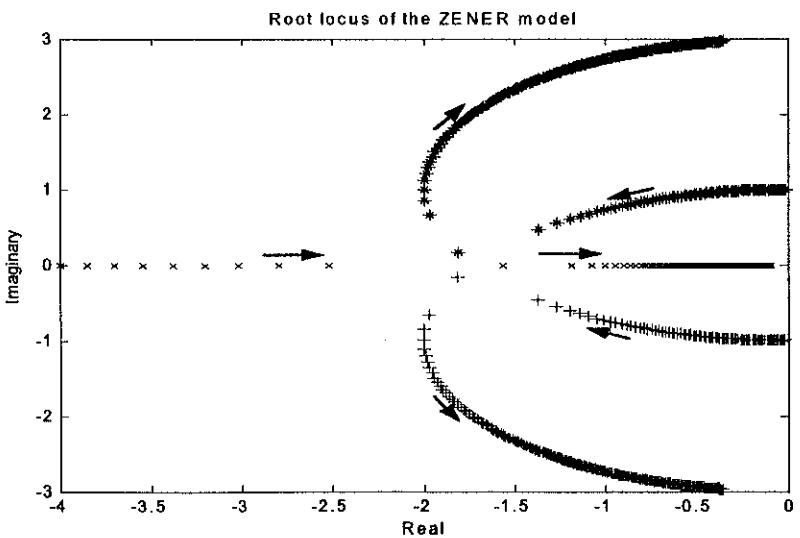

(c)

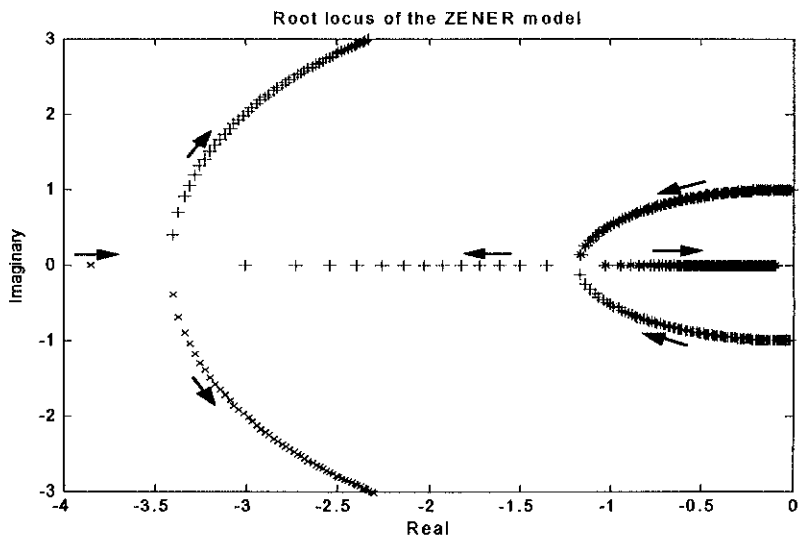

(d)

Figure 7.3. – Root locus diagrams for the Zener model. Note the path followed by the roots s_1 (x), s_2 (+), s_3 (∗) indicated with arrows (a) α=1, (b) α=5, (c) α=8, (d) α=15

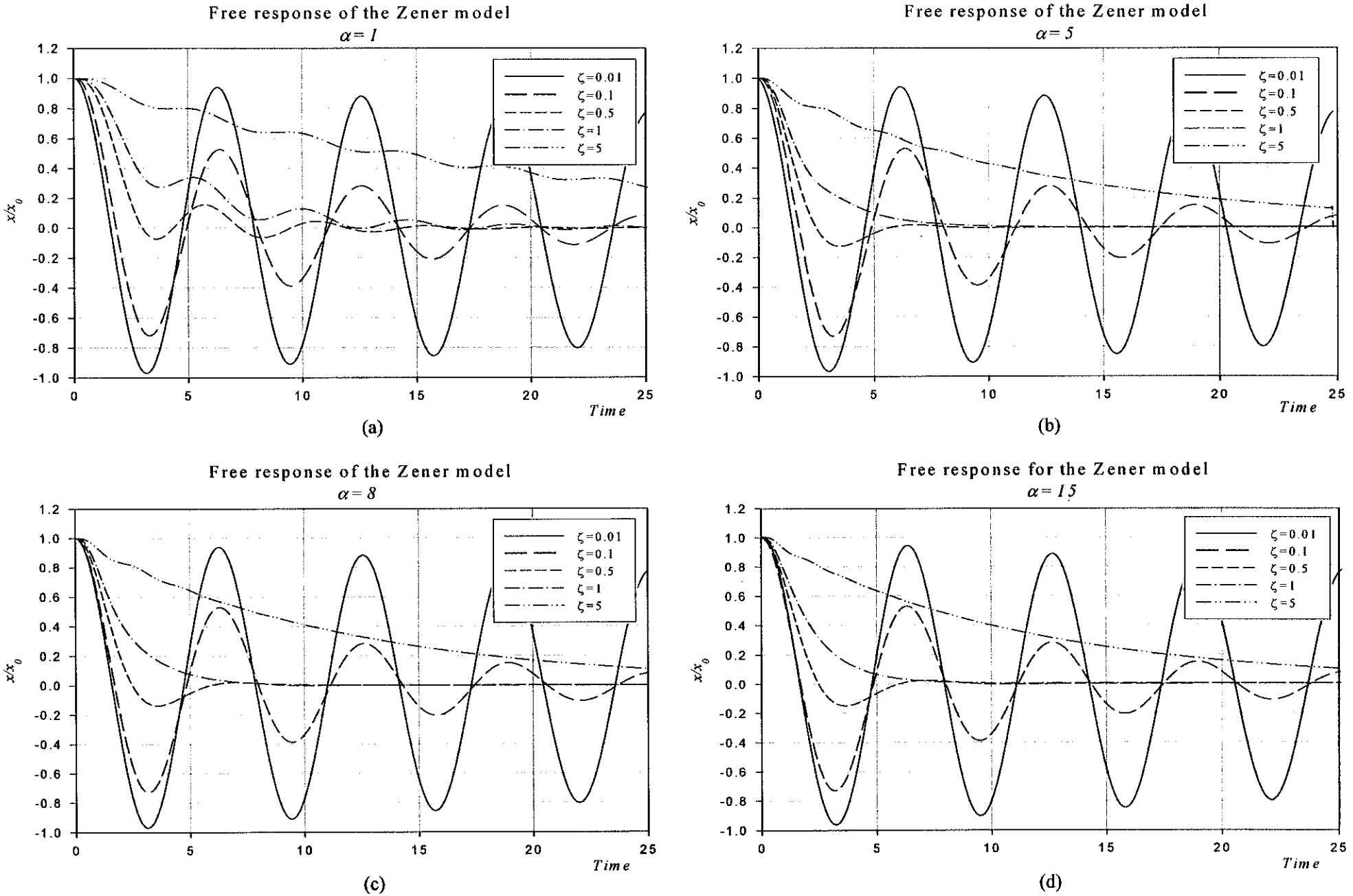

Figure 7.4. – Free response curves for the Zener model, for different values of damping ratio. (a) α=1, (b) α=5, (c) α=8, (d) α=15

8. - HARMONICALLY EXCITED VIBRATION OF THE ZENER MODEL.

For the analysis of the harmonically excited Zener model, a similar procedure to that used in section 7.1 is used. But in this case, a sinusoidal force $F(t)$ acts on the mass. Consider the system shown in figure 8.1.

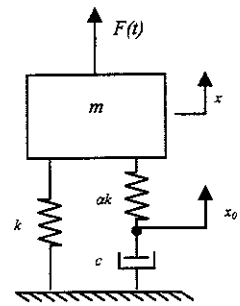

Figure 8.1. - Zener model under the action of a harmonic force.

The equation of motion for the mass can be written as:

$$m\ddot{x} + kx + \alpha k\left(x - x_0\right) = F(t) \tag{8.1}$$

As before one has force equilibrium at the connection point of the damper c and the spring αk:

$$c\dot{x}_0 + \alpha k\left(x - x_0\right) = 0 \tag{8.2}$$

Combining equations 8.1 and 8.2 and differentiating the equation of motion for harmonic excitation one can write:

$$m\dddot{x} + \frac{\alpha km}{c}\ddot{x} + k\left(\alpha + 1\right)\dot{x} + \frac{\alpha k^2}{c}x = \dot{F}\left(t\right) + \frac{\alpha K}{c}F\left(t\right) \tag{8.3}$$

Using equation 6.9, and considering the case when the forcing frequency ω is equal to the transition frequency ω_t[1], the maximum loss factor is given by:

$$\eta_{\max} = \frac{\alpha}{2\sqrt{\left(\alpha + 1\right)}} \tag{8.4}$$

From reference [4], and considering equation 8.4, the transmissibility for the Zener model is given by:

$$T = \frac{\left\{\left[\Omega_n^2 + \Omega_t^2\right]^2 + \left[2\Omega_n\Omega_t\eta_{\max}\right]^2\right\}^{1/2}}{\left\{\left[\Omega_n^2 + \Omega_t^2\right] - \Omega_n^2\left[\Omega_n^2 + \Omega_t^2\left(\alpha + 1\right)\right]\left[\frac{1 + \Omega_t^2}{1 + \Omega_t^2\left(\alpha + 1\right)}\right] + \left[2\Omega_n\Omega_t\eta_{\max}\right]^2\right\}^{1/2}} \tag{8.5}$$

1.- The transition frequency is the characteristic frequency for which the value of loss factor is a maximum. For more details, see appendix C.

Where $\Omega_n = \left(\frac{\omega}{\omega_n}\right), \Omega_t = \left(\frac{\omega_t}{\omega_n}\right)$, and $\omega_n = \sqrt{\frac{k}{m}}$ the natural frequency of the single MKC system.

It is easily seen that transmissibility can be controlled by changing the parameters α and Ω_t (which depends on both the natural and the transition frequencies). In order to investigate the effect of those parameters on the transmissibility, equation 8.5 is plotted for different values of α in figure 8.2. For each plot, several values of Ω_t are considered. Additionally transmissibility curves for the classical MKC are included as a reference, for a system highly damped (ζ=*1* dotted line) and for a system with negligible damping (short dashed line). Additional plots of this system for more values of α can be found in reference [14].

In the low frequency region the behaviour of the system is the same for any value of α and Ω_t, and also is the same as that observed in the classical MKC system. In reference to the resonance region, for all the values of α, when Ω_t =*1* the transmissibility peak is partially suppressed. As long as α increases, the transmissibility peak decreases (the loss factor is directly proportional to α), but this increases the transmissibility at high frequencies It is important to recall that the stiffness increases with frequency too, and this causes a decrement in the isolation efficiency. In general, for small values of damping the behaviour at resonance is similar to highly damped MKC systems. Concerning the response at higher frequencies, the transmissibility decreases rapidly at 40 dB/decade similar to the undamped system, which is twice the MKC system roll off rate (20 dB/decade). However, a larger value of Ω_t will increase the transmissibility in this region.

It is clear that the Zener system presents some advantages over the classical system; however it is necessary to choose the correct parameters for a particular system. The efficiency of the isolation system is a compromise between decreasing the transmissibility at resonance, without compromising the high frequency behaviour. In general, the best results from the graphs presented here seems to be for Ω_t =*1* and $4 \leq \alpha \leq 8$, but this will depend on the characteristics of a particular system. A very good study of the steady state vibration of the Zener model is the work published by Snowdon [4, 15].

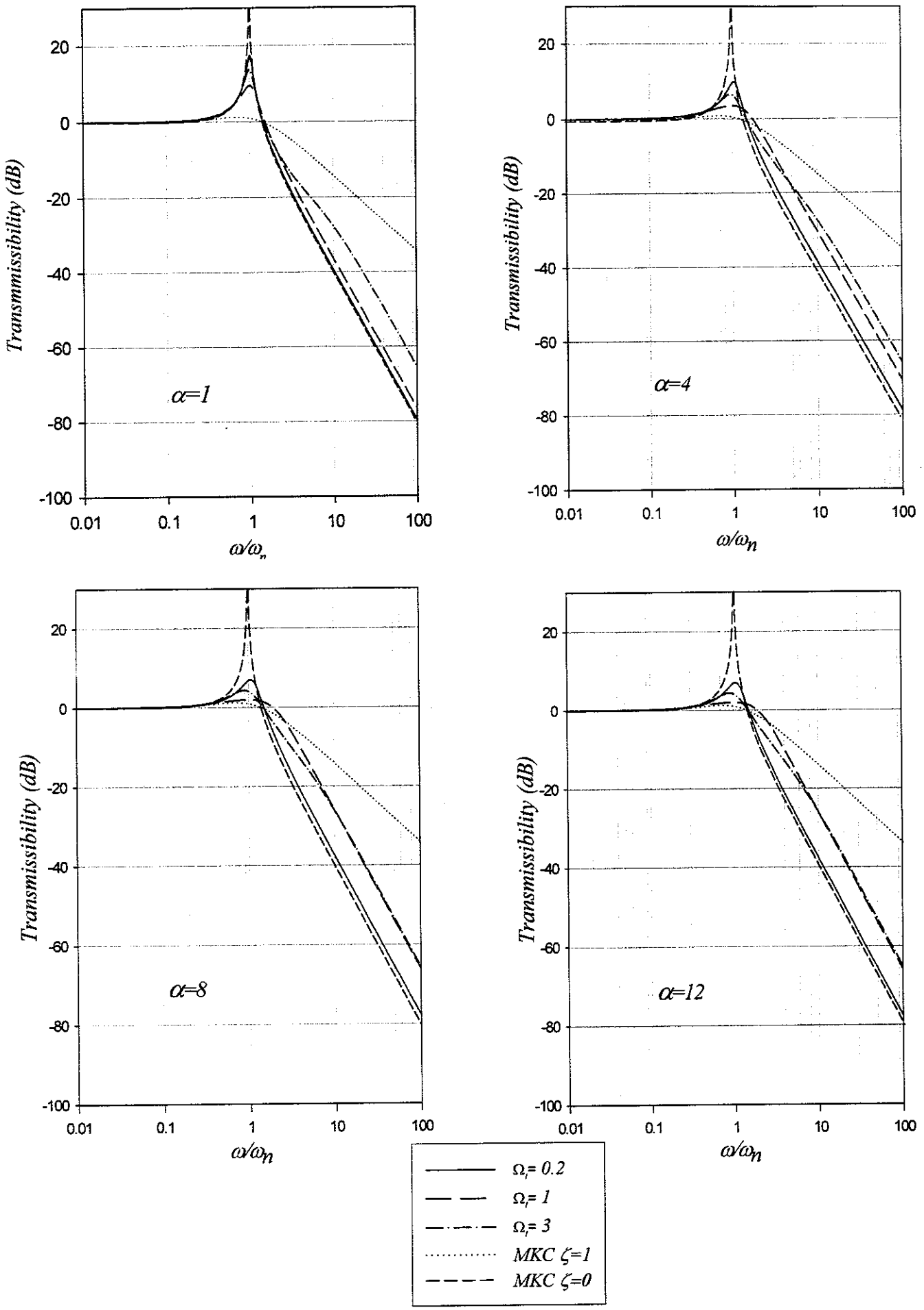

Figure 10. - Transmissibility curves for (a) α=1, (b) α=4, (c) α=8, (d) α=12. Each graph has been produced for different values of M. Curves for MKC system are included

9. - TRANSIENT RESPONSE OF THE ZENER MODEL.

This section is concerned with the analysis of the transient behaviour of the Zener model, particularly due to shock inputs. There are much fewer studies reported on the transient behaviour of this system; a notable exception being the work of Snowdon [15]. In this work the effects of symmetrical pulses are considered, acting as excitation functions. Two different functions will be analyzed; a rectangular pulse and a half sine pulse. The principal objective of this section is to obtain the shock response spectra for maximax response for the different inputs, and compare the performance of this model and the classical MKC model.

9.1. - Equation of motion.

In order to obtain the transient response, a more general form of equation 7.3 will be used, considering the notation used in section 3.1 (table 3.1):

$$m\ddot{v}+\frac{\alpha km}{c}\ddot{v}+k(\alpha+1)\dot{v}+\frac{\alpha k^2}{c}v=\dot{\xi}(t)+\frac{\alpha K}{c}\xi(t) \tag{9.1}$$

In this expression, $\xi(t)$ is a general excitation function, which can be a ground displacement, a ground acceleration, an impulsive force, etc. The term v is the system response stated in a general form. The general analysis of this model is done in terms of maximax response and residual response (see section 2).

Concerning shock inputs, when the excitation function is a pulse one very important parameter is the duration and the shape of that pulse (τ). The system is excited only during that time; afterwards the system is in free vibration. The excitation functions are given by:

Rectangular

$$\begin{cases}\xi(t)=\xi_c & [0\le t\le\tau]\\ \xi(t)=0 & [\tau\le t]\end{cases} \tag{9.2}$$

Half cycle sine

$$\begin{cases}\xi(t)=\xi_c\sin\left(\frac{\pi t}{\tau}\right) & [0\le t\le\tau]\\ \xi(t)=0 & [\tau\le t]\end{cases} \tag{9.3}$$

Where ξ_c is the maximum height of the pulse.

9.2 Shock response spectra.

For this system it is very difficult to obtain analytical expressions for the response. As a result time responses have been obtained numerically using MATLAB, and the spectra has been computed based on the numerical solutions obtained.

9.2.1 Shock response spectra for maximax and residual response.

Shock response spectra for the maximax response are shown in figures 9.1 and 9.2 for half sine and rectangular pulses. The horizontal axis represents the ratio between the duration of the pulse τ and the natural period of the system T, while the vertical axis represents the maximax response v_m normalized with respect to the pulse height ξ_c (this value is also called magnification factor and it is analogous to the transmissibility). The graphs have been produced for four different values of α (1, 5, 8, and 15). Furthermore, each graph comprises various values of damping ratio, and the curves for the classical MKC system have been included as a reference.

Inspecting figure 9.1 for the half sine pulse, it is easily seen that for the classical system the maximum possible value of v_m/ξ_c is approximately 1.79, and only when τ/T is very small (less than 0.5) v_m/ξ_c can be smaller than 1. As τ/T increases, the ratio v_m/ξ_c tends to approach 1, no matter the amount of damping present in the system. The response then is quasi static and it follows closely the shape of the pulse. In summary, isolation is only possible for a small range of values of τ/T . Also, for the Zener model one can observe that this model exhibits a very similar behaviour for all values of α. The value of α does not cause significant changes in the spectra. Only for α=1 the is spectrum slightly different, and for the other values it shows almost the same behaviour (excluding the cases for very small α and very large α which represents the cases of a single mass spring system and a mass spring damper in parallel system respectively.).

Figure 9.2 shows the maximax spectra for a rectangular pulse. In this case the limiting values for the classical system are 1 and 2. For the Zener system the behaviour is very similar to when the input is the half sine pulse. In general a decrease of the response can be achieved as a result of larger values of damping and larger values of α. The advantage over the classical system can only be observed for $\alpha \geq 15$, however this advantage is of no significance and it does not justify the complexity of the model, at least for passive shock isolation. Spectra for the residual response for both half sine and rectangular functions are shown in figures 9.3 and 9.4 respectively. Spectra for the classical highly damped MKC system and the MK system are included as well. In reference to the MK system, it is possible to get zero residual response for certain values of τ/T . Concerning the half sine pulse, for the Zener system

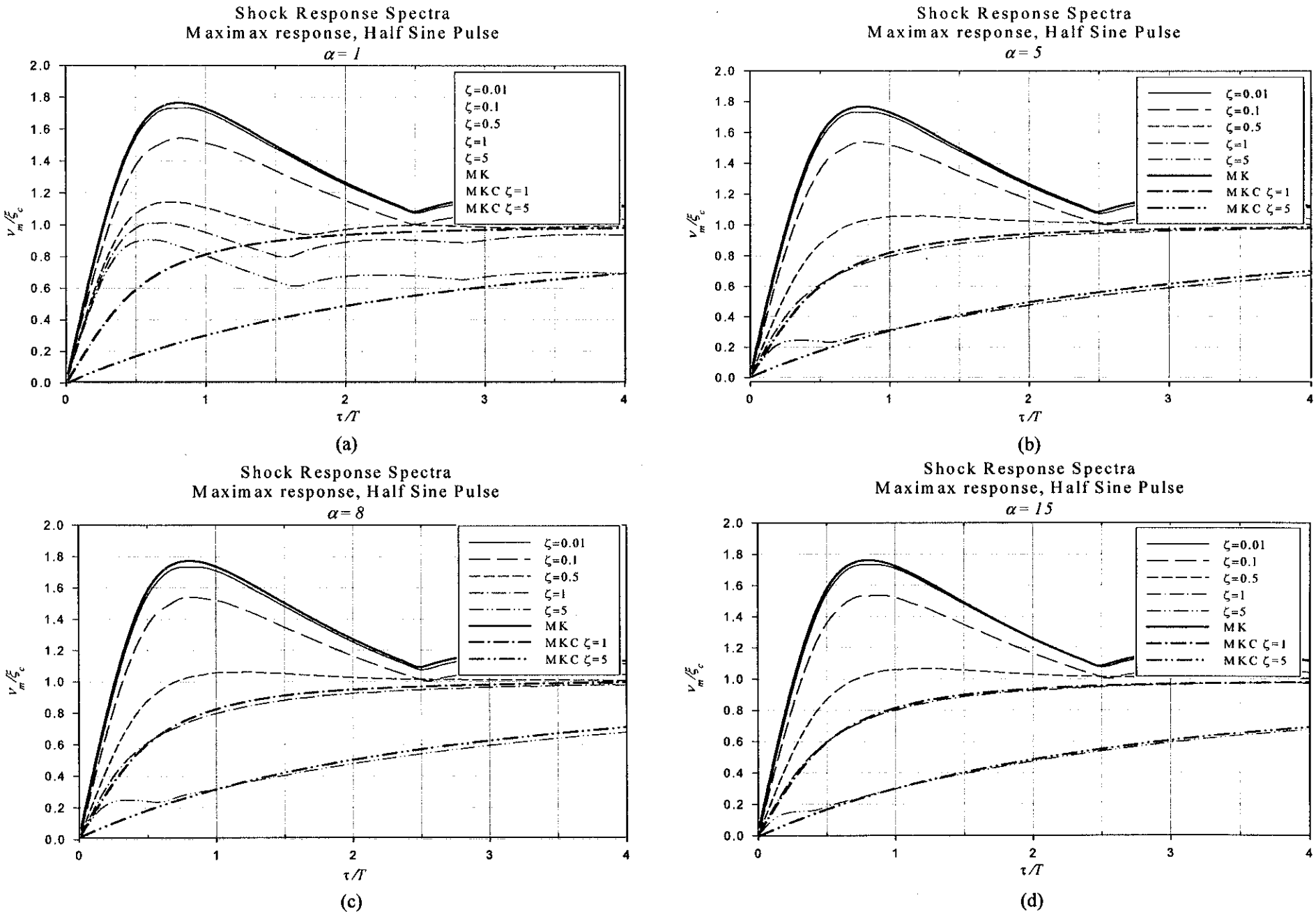

Figure 9.1.- Shock response spectra for maximax response of the Zener model, for half sine excitation. Bold lines represent the spectra for the MKC system with ζ=1 and ζ=5,and MK system. (a) α=1, (b) α=5, (c) α=8, (d)α=15

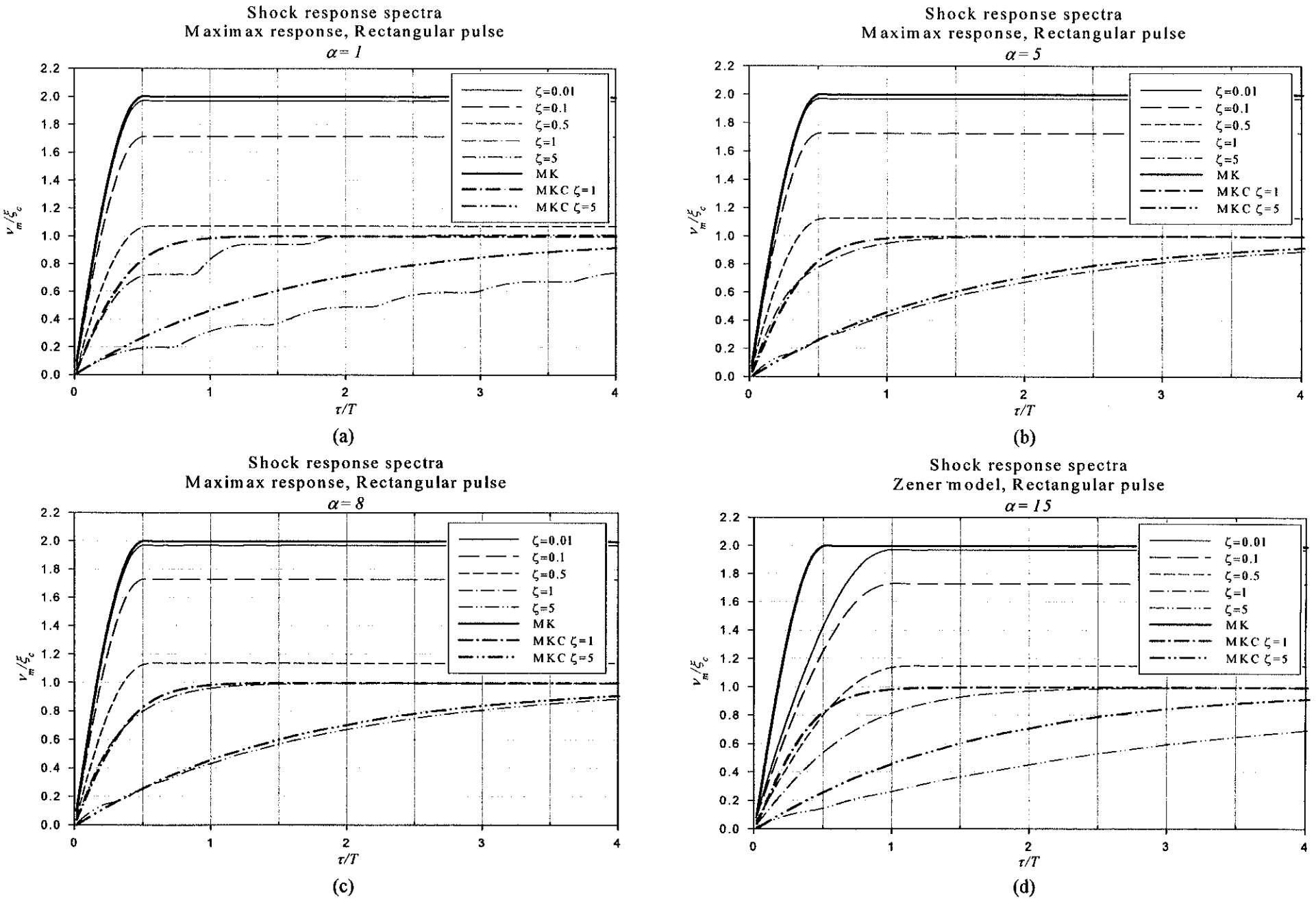

Figure 9.2.- Shock response spectra for maximax response of the Zener model, for rectangular pulse excitation. Bold lines represent the spectra for the MKC system with ζ=1 and ζ=5,and MK system. (a) α=1, (b) α=5, (c) α=8, (d)α=15

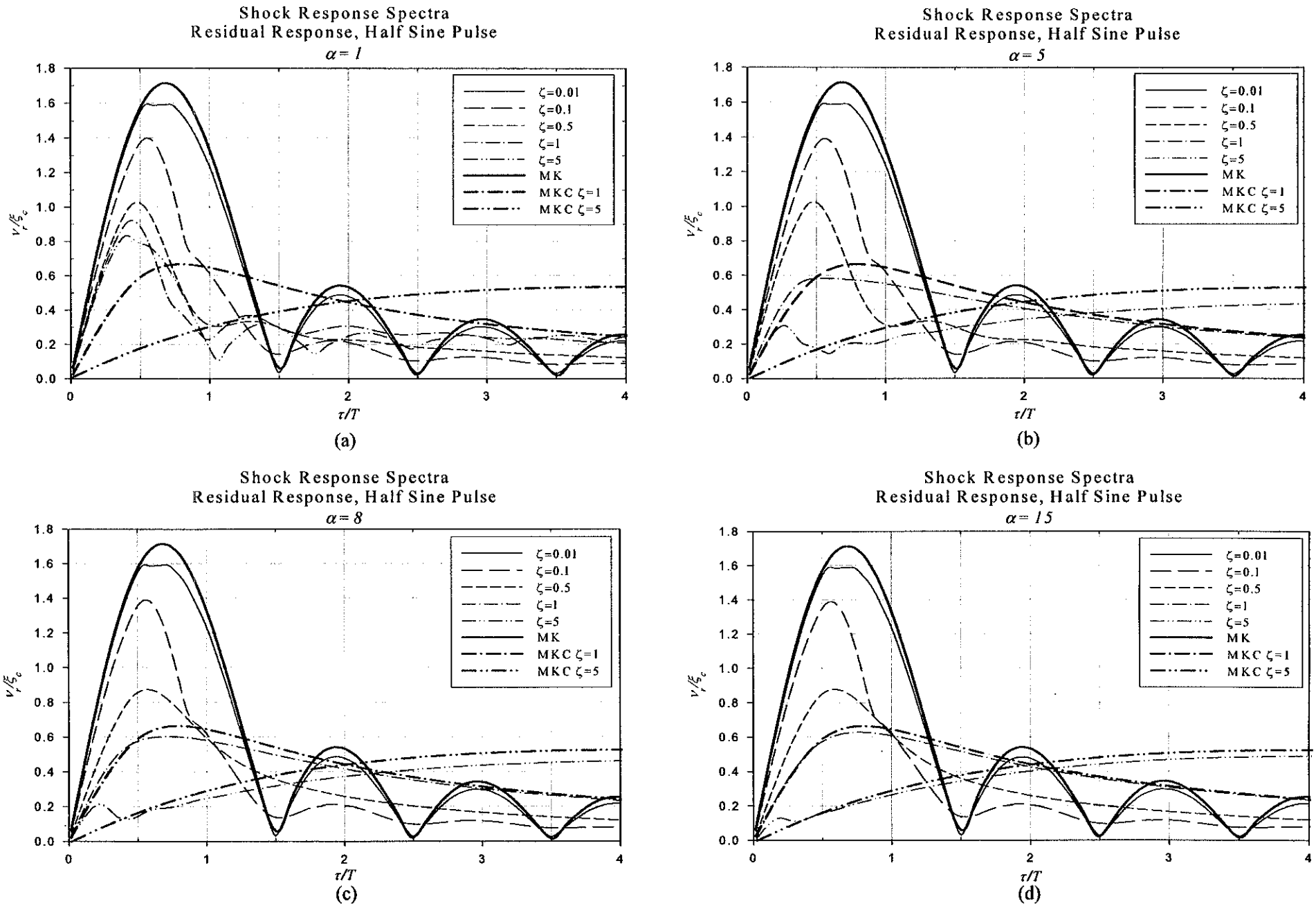

Figure 9.3.- Shock response spectra for residual response of the Zener model, for half sine excitation. Bold lines represent the spectra for the MKC system with ζ=1 and ζ=5,and MK system. (a) α=1, (b) α=5, (c) α=8, (d)α=15

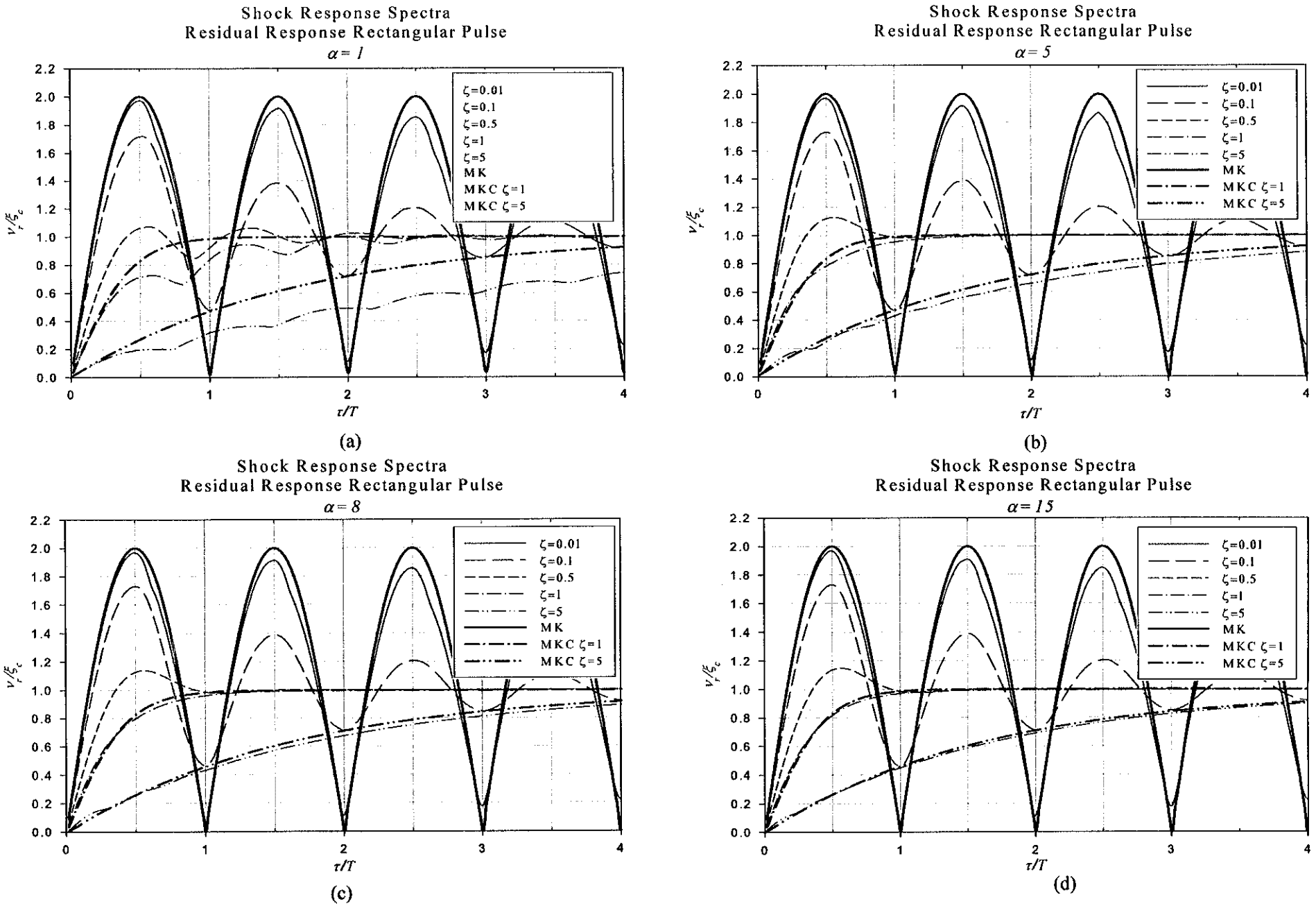

Figure 9.4.- Shock response spectra for residual response of the Zener model, for rectangular pulse excitation. Bold lines represent the spectra for the MKC system with ζ=1 and ζ=5,and MK system. (a) α=1, (b) α=5, (c) α=8, (d)α=15

this is only possible for small values of damping, however, the overall values of residual response are similar to those observed in the classical system. As the damping ratio increases the system residual response increases too, but it tends to decrease to zero for larger values of τ/T, as the system becomes quasi static. In general the curves for the Zener model follow closely the spectra of the classical system. However a small decrease of the magnification factor is obtained using the Zener model.

For the rectangular pulse, a similar behaviour is observed for all values of α. In this case it is not possible for the Zener model to have zero residual response. In general the value of residual response can be decreased for high damping levels; however for large values of τ/T the residual response tends to be equal to the height of the pulse for any value of damping ratio.

For a better understanding of the effect of the pulse period and shape on both maximax and residual response the reader can refer to appendix 3. This appendix comprises a comprehensive set of time histories for the Zener model. The figures are given for α=1 and 8. The behaviour observed is similar for values of α higher than 4. For each value of α solution curves have been computed for ζ=0.1, 0.5 and 1, and each curve represents a different value of τ/T. For half sine excitation, in most of the cases for values of τ/T less than 0.5 the maximax response occurs after the excitation has finished (maximax and residual response are the same). It is important to point out that for equal values of damping ratio, the larger the value of α, the smaller is the response, however, the reduction in the response is small. Additionally, for larger values of α the system reaches the equilibrium position with fewer oscillations. In reference to the rectangular pulse, the maximax response is observed after the pulse has finished for values of τ/T less than 0.5 for any value of α and damping ratio. The overall behaviour is analogous to that observed in the half sine case.

Further understanding regarding the effect of damping on the Zener model can be achieved by considering the results shown in figure 9.5. This figure is a comparison of the effect of damping on limiting the maximax response for different values of α. The comparison is given for both half sine and rectangular pulses. The maximax for the classical MK system has been taken as a reference. This graph clearly shows that in both cases the behaviour is almost the same for the MKC system and for the Zener model apart from for small values of α in the case of half sine excitation. In this situation the performance of the system diminishes. For the rectangular pulse a small reduction on maximax response is gained, but only for small values of α and high values of damping (greater than 1).

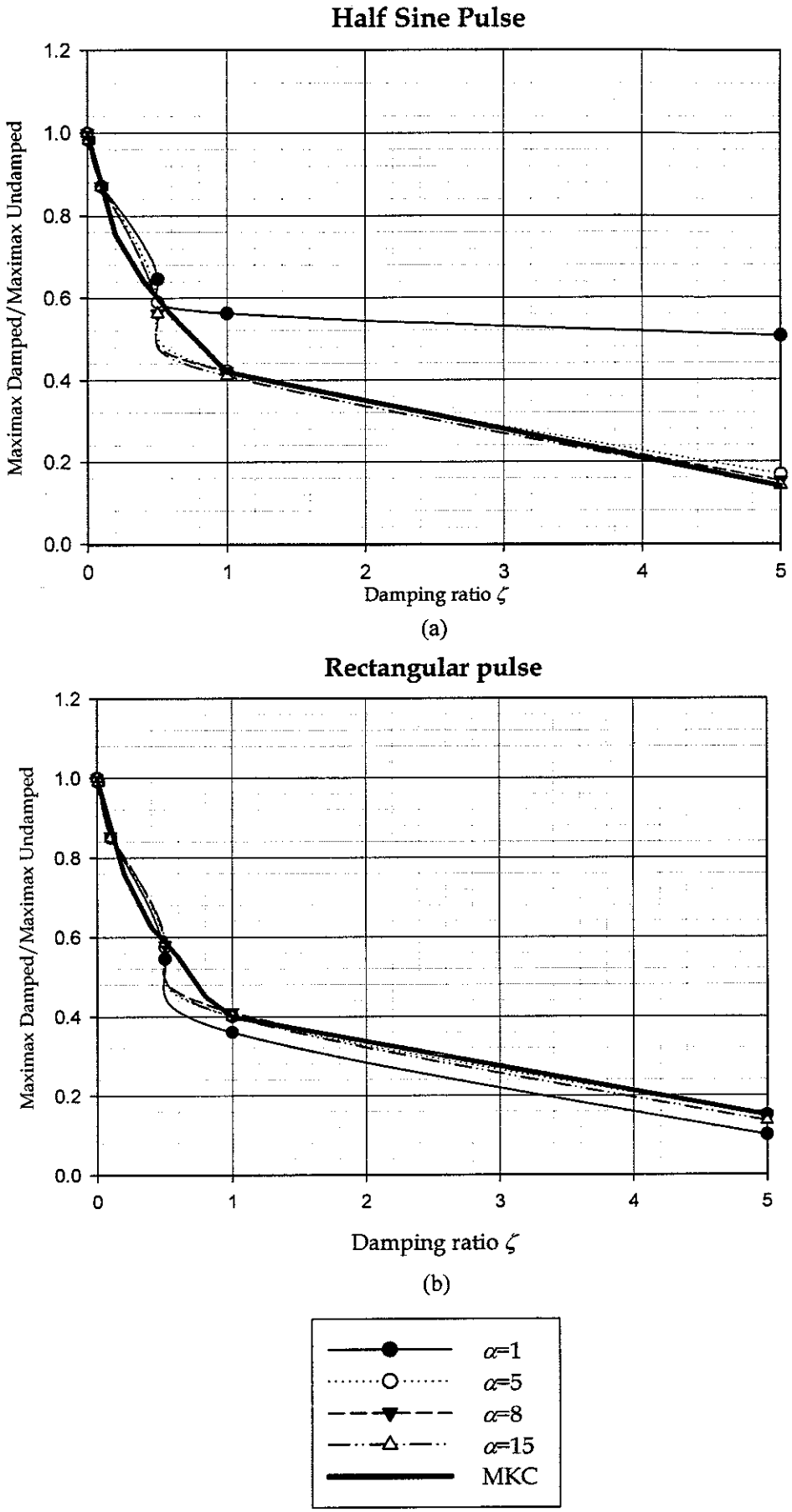

Figure 9.5 . – Effect of damping ratio on limiting maximax response in the Zener model. The maximax for the undamped classical system has been taken as a reference. (a) Half sine pulse, (b) Rectangular pulse

10. - CONCLUSIONS.

The most important quantities in shock measurements are the maximax response and the residual response, both used to determine the severity of the shock. A powerful tool in the analysis of shock motions is the *shock response spectrum,* which gives information about the relationship between the maximax response and the duration of the shock and the natural period of the system.

From the undamped system shock response spectrum and time responses for step functions, it is clear that the maximax response always occurs after the excitation has reached its maximum. On the other hand, for pulse inputs, the response depends upon the ratio of the duration of the pulse to the natural period of the system. If the pulse is of short duration, the shape of the pulse is not important (for τ/T less than 0.5), and the maximax occurs after the excitation has ceased. In contrast, when the pulse is long, the shape plays an important role and maximax response can occur during the pulse, or after it has ceased. For some values of τ/T, the residual response is zero.

The acceleration as a response quantity is another parameter considered in this work. Accordingly with previous studies [4] the acceleration was found to be the most important parameter when the duration of the pulse is long compared to the natural period, but the displacement is more important when the pulse is of short duration.

Inclusion of viscous damping in the system generally results in a decrease in the maximax response and residual response. Nevertheless, the effect of damping is not of great significance unless the system is highly damped. Furthermore, when the acceleration response is analyzed as a result of a base displacement, large amounts of damping will cause high levels of acceleration during the shock input. Lower overall levels of acceleration are observed for $0.2 \leq \zeta \leq 0.3$

Most of the work has been carried out considering only the classical MKC system which is the simplest mathematical representation of a damped system and includes a dashpot (viscous damper) in parallel with an elastic spring. However, this approach does not represent very well real systems. In practice, many materials present viscoelastic behaviour where one of the most important characteristics of the viscoelastic phenomenon is the frequency dependence of the stiffness and damping.

The simplest representation of viscoelastic behaviour is the mathematical model known as Zener model. This system comprises a dashpot elastically connected, arranged in parallel to another elastic spring. The model is not an exact representation of viscoelastic materials, but it provides a very good approximation using a relatively simple system. This system shows the

frequency dependence characteristic of viscoelastic materials, having a transition frequency, in which the damping takes its maximum value.

In general the Zener model shows a better performance over the classical MKC system only for one of the three conditions considered, namely harmonically excited vibration. For harmonic excitation, the system has the characteristics of a highly damped MKC system, plus a reduction of the transmissibility at higher frequencies due to the frequency dependence of the stiffness and the loss factor. In the case of shock excitation, the improved performance of the Zener model over the classical MKC system is not so apparent, showing only small benefits in shock isolation for certain values of α and highly damped systems. However, this system can be used in certain systems under both transient and harmonically excited disturbances where it could be promising.

This work can be extended by considering the response for different input functions in the case of shock excitation for the Zener model. Moreover, the effect of non linear elements (spring, dashpot, or both) could be investigated. Little information has been published for the possible non linearity in the Zener model [13]. Future alternatives might be to consider the implementation of adaptive or semi active vibration control since little work has been done in this area for shock excitation. A low stiffness mount could be promising for shock isolation since the isolation occurs only for low natural frequencies. This would cause large deformations in the elastic element that will provide high levels of energy stored. However, it is not possible to reduce the stiffness below a certain point because the mount has to be stiff enough to support the system statically. Moreover, the free space for a large deformation can be a restraint. A future work could include the possibilities of developing an active or adaptive suspension that will become "soft" during the impact to minimize the response.

Appendix A

Solution of the equations of motion using Laplace transformations.

a) Constant slope step.

The equation of motion is given by:

$$\frac{\ddot{v}}{\omega_n^2} + v = \xi(t) \qquad \text{a1}$$

Where:

$$\xi(t) = \begin{cases} \xi_c \dfrac{t}{\tau} & [0 \le t \le \tau] \\ \xi_c & [\tau \le t] \end{cases} \qquad \text{a2}$$

Taking the Laplace transformation of equation a1:

$$\frac{1}{\omega_n^2}\left(s^2 v(s) - s v_0 - s\dot{v}_0\right) + v(s) = \xi(s) \qquad \text{a3}$$

Considering that the system is initially at rest and rearranging equation a3:

$$v(s) = \frac{\omega_n^2 \xi(s)}{s^2 + \omega_n^2} \qquad \text{a4}$$

The solution of the equation of motion is given by the inverse transformation of equation a4. From [19], the transformation $\xi(s)$ for this particular case is given by:

$$\xi(s) = \frac{\xi_c}{\tau}\frac{1 - e^{s\tau}}{s^2} \qquad \text{a5}$$

As a result, and after an algebraic manipulation of equations a4 and a5, the solution is given by:

$$v(t) = \frac{\xi_c}{\tau}\omega_n^2 \mathcal{L}^{-1}\left[\frac{1}{s^2\left(s^2 + \omega_n^2\right)} - \frac{e^{-s\tau}}{s^2\left(s^2 + \omega_n^2\right)}\right] \qquad \text{a6}$$

Using Laplace transform pairs from [1] and [19], the response is given by:

$$v(t) = \frac{\xi_c}{\omega_n \tau}\left[\omega_n t - \sin(\omega_n t) - \left(\omega_n(t-\tau) - \sin\omega_n(t-\tau)\right)\right] \qquad \text{a7}$$

Using $\sin(A+B)-\sin(A-B)=2\cos A\sin B$ to simplify equation a7 one can write:

$$v(t)=\begin{Bmatrix}\dfrac{\xi_c}{\omega_n\tau}\left[\omega_n t-\sin(\omega_n t)\right] & 0\le t\le\tau\\ \xi_c\left[1+\dfrac{1}{\omega_n\tau}\left(2\sin\left(\dfrac{\omega_n\tau}{2}\right)\cos\omega_n\left(t-\dfrac{\tau}{2}\right)\right)\right] & \tau\le t\end{Bmatrix}$$

a8

From the response when $\tau\le t$, the maximax response is given by the following expression, since it is a constant amplitude value:

$$v_m=\xi_c\left[1+\frac{2}{\omega_n\tau}\left(\sin\left(\frac{\omega_n\tau}{2}\right)\right)\right] \qquad \text{a9}$$

Finally, considering that $\omega_n=\dfrac{2\pi}{T}$ and rearranging equation a9:

$$\frac{v_m}{\xi_c}=1+\frac{T}{\pi\tau}\left(\sin\left(\frac{\pi\tau}{T}\right)\right) \qquad \text{a10}$$

Equation a10 gives the normalized maximax response as a function of the ratio.

b) Rectangular pulse.

This is the case of a symmetrical pulse. The forcing function is given by:

$$\xi(t)=\begin{Bmatrix}\xi_c & 0\le t\le\tau\\ 0 & \tau\le t\end{Bmatrix} \qquad \text{a11}$$

The Laplace transform of the forcing function is given by [1]:

$$\xi(s)=\xi_c\frac{1-e^{s\tau}}{s} \qquad \text{a12}$$

From the previous analysis one can take directly equation a4 and combine with equation a12 in order to obtain the solution. The solution is given by:

$$v(t)=\xi_c\omega_n^2\mathcal{L}^{-1}\left[\frac{1}{s^2\left(s^2+\omega_n^2\right)}-\frac{e^{-s\tau}}{s^2\left(s^2+\omega_n^2\right)}\right] \qquad \text{a13}$$

The inverse transform of equation a13 is:

$$v(t) = \xi_c\left[1 - \cos(\omega_n t) - (1 - \cos\omega_n(t-\tau))\right] \qquad \text{a14}$$

Using $\cos(A-B) - \cos(A+B) = 2\sin A \sin B$, one can rewrite equation a14 as follows:

$$v(t) = \begin{cases} \xi_c\left[1 - \cos(\omega_n t)\right] & 0 \le t \le \tau \\ \xi_c\left[2\sin\left(\dfrac{\omega_n \tau}{2}\right)\sin\omega_n\left(t - \dfrac{\tau}{2}\right)\right] & \tau \le t \end{cases} \qquad \text{a15}$$

The amplitude term of the residual era can be written in terms of the natural period and one can write an expression for the residual response as:

$$\frac{v_r}{\xi_c} = \left[2\sin\left(\frac{\pi\tau}{T}\right)\right] \qquad \text{a16}$$

By differentiating this term with respect to τ/T and equaling it to zero, the obtained value of $\tau/T = 1/2$ is evaluated in equation a16 in order to obtain the maximax response, given by:

$$\frac{v_m}{\xi_c} = 2 \qquad \text{a17}$$

This is valid for $\tau/T \ge 1/2$. For lower values, the residual response is equal to the maximax response.

c) Half sine pulse.

The forcing function is given by:

$$\xi(t) = \begin{cases} \xi_c \sin\left(\dfrac{\pi t}{\tau}\right) & [0 \le t \le \tau] \\ 0 & [\tau \le t] \end{cases} \qquad \text{a18}$$

The Laplace transform of the forcing function is [1]:

$$\xi_c \frac{\pi/\tau}{s^2 + (\pi/\tau)^2}\left(1 + e^{-s\tau}\right) \qquad \text{a19}$$

From equation a4 and a19, after an algebraic manipulation one can write:

$$v(t)=\xi_c\frac{\pi}{\tau}\omega_n^2\mathcal{L}^{-1}\left[\frac{1}{\left(s^2+\omega_n^2\right)\left(s^2+\left(\pi/\tau\right)^2\right)}\right]+\mathcal{L}^{-1}\left[\frac{e^{-s\tau}}{\left(s^2+\omega_n^2\right)\left(s^2+\left(\pi/\tau\right)^2\right)}\right] \qquad \text{a20}$$

Using Laplace transforms pairs given by [1], the solution of the equation can be expressed as follows:

$$v(t)=\xi_c\frac{\pi}{\tau}\omega_n^2\left[\frac{\omega_n\sin\left(\frac{\pi}{\tau}t\right)-\frac{\pi}{\tau}\sin\left(\omega_n t\right)}{\frac{\omega_n\pi}{\tau}\left(\omega_n^2+\frac{\pi^2}{\tau^2}\right)}+\frac{\omega_n\sin\frac{\pi}{\tau}\left(t-\tau\right)-\frac{\pi}{\tau}\sin\omega_n\left(t-\tau\right)}{\frac{\omega_n\pi}{\tau}\left(\omega_n^2+\frac{\pi^2}{\tau^2}\right)}\right] \qquad \text{a21}$$

Simplification of equation a21 leads to:

$$\left\{\begin{array}{ll} v(t)=\dfrac{\xi_c}{1-T^2/4\tau^2}\left(\sin\left(\dfrac{\pi t}{\tau}\right)-\dfrac{T}{2\tau}\sin\omega_n t\right) & \left[0\le t\le\tau\right] \\ v(t)=\xi_c\left[\dfrac{\left(T/\tau\right)\cos\left(\pi\tau/T\right)}{\left(T^2/4\tau^2\right)-1}\right]\sin\omega_n\left(t-\dfrac{\tau}{2}\right) & \left[\tau\le t\right] \end{array}\right\} \qquad \text{a22}$$

Appendix B

Proof of zero residual response for symmetrical pulses.

In the case of symmetrical pulses acting on the mass spring system, for certain values of the ratio τ/T there is no residual response (see figure 3.5) that means the system is at rest when the pulse has finished. The reason behind this happening is the fact that the total work done by the forcing function is equal to zero for the corresponding value of τ/T. The work done during the shock period can be defined as:

$$\int_0^{\tau} \xi(t)\,dx = \int_0^{\tau} \xi(t)\frac{dt}{dx}\,dx \qquad \text{b1}$$

a) Rectangular pulse.

The forcing function is given by:

$$\xi(t) = \begin{cases} \xi_c & 0 \le t \le \tau \\ 0 & \tau \le t \end{cases} \qquad \text{b2}$$

And the response during the impulse is:

$$x(t) = \xi_c\left[1-\cos(\omega_n t)\right] \qquad \text{b3}$$

The velocity is obtained by differentiating equation b3 as follows:

$$\frac{dx}{dt} = \omega_n \xi_c \sin(\omega_n t) \qquad \text{b4}$$

Equations b2 and b4 are substituted in equation b1 to obtain the following expression:

$$\omega_n \xi_c^2 \int_0^{\tau} \sin(\omega_n t)\,dt \qquad \text{b5}$$

After evaluating the integral one can write the expression for the total work done by the force.

$$\xi_c^2\left[\cos\left(\frac{2\pi\tau}{T}\right)-1\right] \qquad \text{b6}$$

From figure 3.5 one can see that residual response is zero when $\tau/T = 1,2,3...$ by evaluating these values in equation b6 it is readily seen that the total work done is zero.

b) **Half sine pulse.**

In this case the forcing function can be written as follows:

$$\xi(t)=\begin{cases}\xi_c \sin\left(\dfrac{\pi t}{\tau}\right) & [0\le t\le \tau] \\ 0 & [\tau\le t]\end{cases} \qquad \text{b7}$$

The displacement of the mass and its corresponding velocity during the disturbance period are given by:

$$x=\frac{\xi_c}{1-T^2/4\tau^2}\left(\sin\left(\frac{\pi t}{\tau}\right)-\frac{T}{2\tau}\sin\left(\frac{2\pi t}{T}\right)\right) \qquad \text{b8}$$

$$\frac{dx}{dt}=\frac{4\xi_c\pi\tau}{4\tau^2-T^2}\left(\cos\left(\frac{\pi t}{\tau}\right)-\cos\left(\frac{2\pi t}{T}\right)\right) \qquad \text{b9}$$

Substituting equation b9 and b7 in the integral given by equation b1:

$$\frac{4\xi_c\pi\tau}{4\tau^2-T^2}\int_0^{\tau}\sin\left(\frac{\pi t}{\tau}\right)\left(\cos\left(\frac{\pi t}{\tau}\right)-\cos\left(\frac{2\pi t}{T}\right)\right)dt \qquad \text{b10}$$

The expression for the total work is obtained after performing the previous integral and one can obtain the next expression:

$$\frac{4\xi_c\pi\tau}{4\tau^2-T^2}\left[\frac{\tau^2\left(\cos\left(\frac{2\pi\tau}{T}\right)+1\right)}{\pi(T+2\tau)}-\frac{\tau^2\left(\cos\left(\frac{2\pi\tau}{T}\right)+1\right)}{\pi(T-2\tau)}-\frac{\tau\left(\cos\left(\frac{2\pi\tau}{T}\right)+1\right)}{\pi}\right] \qquad \text{b11}$$

From figure 3.5 concerning to the half sine pulse the residual response is zero for $\tau/T=1.5, 2.5, 3.5....$ Evaluating equation b11 at any of these values the total work done by the force is equal to zero.

Appendix C

Frequency dependence of the damping and the stiffness.

This section is concerned with the examination of the dynamic properties of the Zener model. The principal characteristic of this model is that both damping and stiffness are highly frequency dependant. In order to show this behaviour the approach of complex stiffness will be used, as shown in figure 6.1. The objective is to represent the characteristics of the Zener model as a single complex stiffness.

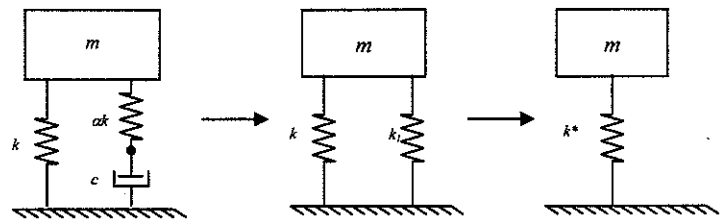

Figure 6.1. - Zener model represented as a single complex stiffness system.

Considering for harmonic motion that $c\dot{x} = j\omega cx$, and arranging the dashpot in series with the spring αk one can write:

$$k_1 = \frac{j\omega c\alpha k}{j\omega c + \alpha k} \tag{c1}$$

Now, k_1 is in parallel with k, which gives:

$$k_{eff} = \frac{j\omega c\alpha k + k(j\omega c + \alpha k)}{j\omega c + \alpha k} \tag{c2}$$

Equation 6.2 can be simplified to:

$$k_{eff} = \frac{k + jk(\alpha + 1)\left(\frac{\omega c}{\alpha k}\right)}{1 + j\left(\frac{\omega c}{\alpha k}\right)} \tag{c3}$$

This finally leads to the complex stifness:

$$k^* = \frac{k + k(\alpha + 1)\left(\frac{\omega c}{\alpha k}\right)^2}{1 + \left(\frac{\omega c}{\alpha k}\right)^2} + j\frac{\omega c}{1 + \left(\frac{\omega c}{\alpha k}\right)^2} \tag{c3}$$

As explained in section 5.2, the real part of the complex stiffness represents the dynamic stiffness k_d of the system, given by:

$$k_d = \frac{k + k(\alpha+1)\left(\frac{\omega c}{\alpha k}\right)^2}{1+\left(\frac{\omega c}{\alpha k}\right)^2} \tag{c4}$$

And the ratio of the imaginary to the real part represents the loss factor η, given by:

$$\eta = \frac{\omega c}{k + k(\alpha+1)\left(\frac{\omega c}{\alpha k}\right)^2} \tag{c5}$$

For viscoelastic materials it has been observed [4, 7 and 9] that the real part of the complex stiffness is constant at low frequencies, it passes through an inflexion point and then reaches a new constant value at high frequencies. On the other hand, the loss factor is small at low frequencies, increasing proportionally with frequency, reaching a maximum value, and then decreases inversely with frequency. The value of frequency for which the loss factor is maximum is called the *transition frequency* ω_t. Although the Zener model does not represent the exact behaviour of viscoelastic materials, it offers a very good approximation. For the Zener model, in order to obtain this transition frequency, it is necessary to solve the equation:

$$\frac{d\eta}{d\omega} = 0 \tag{c6}$$

This gives the following expression for the transition frequency:

$$\omega_t = \frac{\alpha k}{c\sqrt{\alpha+1}} \tag{c7}$$

Equations 6.4 and 6.5 can be rearranged using equation 3.6 to obtain:

$$k_d = \frac{k(\alpha+1)\left[1+\left(\frac{\omega}{\omega_t}\right)^2\right]}{(\alpha+1)+\left(\frac{\omega}{\omega_t}\right)^2} \tag{c8}$$

$$\eta = \frac{\alpha\left(\frac{\omega}{\omega_t}\right)}{\sqrt{\alpha+1}\left[1+\left(\frac{\omega}{\omega_t}\right)^2\right]} \tag{c9}$$

Equations 6.8 and 6.9 are shown graphically in figure 6.2 for various values of α. where the real dynamic stiffness is normalized by the value of stiffness equal to $k(\alpha+1)$ Figure 6.2(a) shows the frequency dependence of the dynamic stiffness. By examination of this figure and the analytical expression in (3.8), one can observe that in the low frequency region the dynamic stiffness tends to approach a constant value equal to the value of the spring k. After passing through an inflection point, at higher frequencies the normalized stiffness reaches a constant value of 1 for all values of α. In this case, the dashpot becomes virtually a rigid link and the actual stiffness is equal to the spring k and αk in parallel which is equal to $(k+\alpha k)$ [4]. On the other hand, the loss factor is small at low and high frequencies, but at a certain point it reaches a maximum value, at the transition frequency.

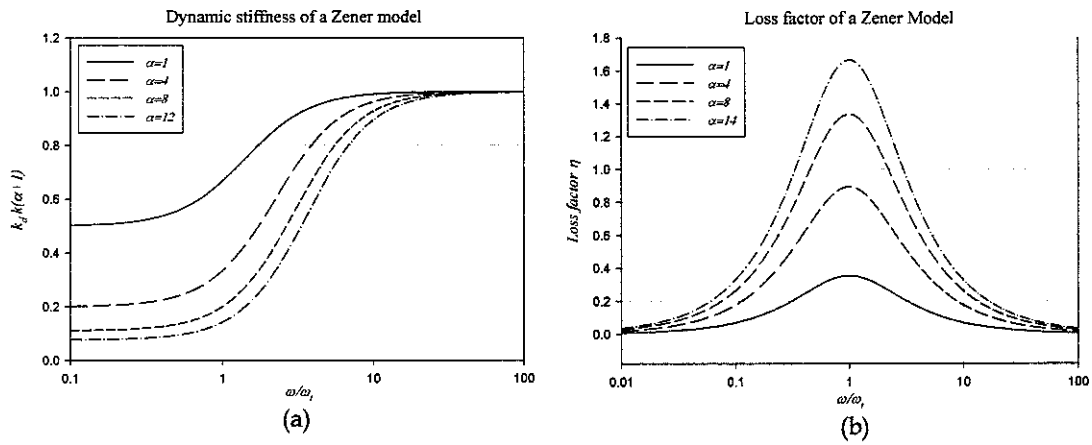

Figure 6.2.- Frequency dependence of the stiffness (a) and the loss factor (b) of the Zener model for different values of α. Note that in the case of (a) the stiffness has been normalized with respect to the high frequency value of the stiffness.

Appendix D

Root locus significance for a single degree of freedom system.

When investigating the free response of mechanical systems a very useful tool is the *root locus* diagram. This plot shows the path followed by the roots of the characteristic equation of a system when a particular parameter is varied from very small to very large values. The roots are plotted in the *complex plane*, or *s-plane*. When the roots are plotted in this way, inspection of the plot reveals the nature of the free response of the system [13]. If the roots are located in the left hand side of the diagram, the system is said to be *stable*. Making the assumption that the system is stable, one can find a different behaviour depending on the location of the roots. If the roots are imaginary, the system oscillates in a sinusoidal manner with constant amplitude. If the roots are real and negative, the system decays to zero as t approaches infinity, with no oscillations. When the roots are complex, the system decays sinusoidally with a exponential envelope. On the other hand, when the roots are on the right half side of the diagram, the system is unstable. The amplitude increases without bound. For mechanical systems this situation appears as a result of *negative damping*, due to phenomena such as chatter in machine tools, or flutter. Consider the characteristic equation of a MKC system.

$$s^2 + 2\zeta\omega_n s + \omega_n^2 = 0 \qquad \text{(d1)}$$

Where ζ is the damping ratio and ω_n is the natural frequency. Note that this equation is of second order, so it has two roots s_1 and s_2. For higher order systems, the response is built up of those functions that include the free response of first and second order systems [13].

As stated before, the nature of the roots gives the behaviour in free response of the system. In this particular case is interesting to look at the behaviour of the roots when the damping ratio varies. Three of the most significant cases are shown in figure d1. Additional information regarding this topic can be found in [13].

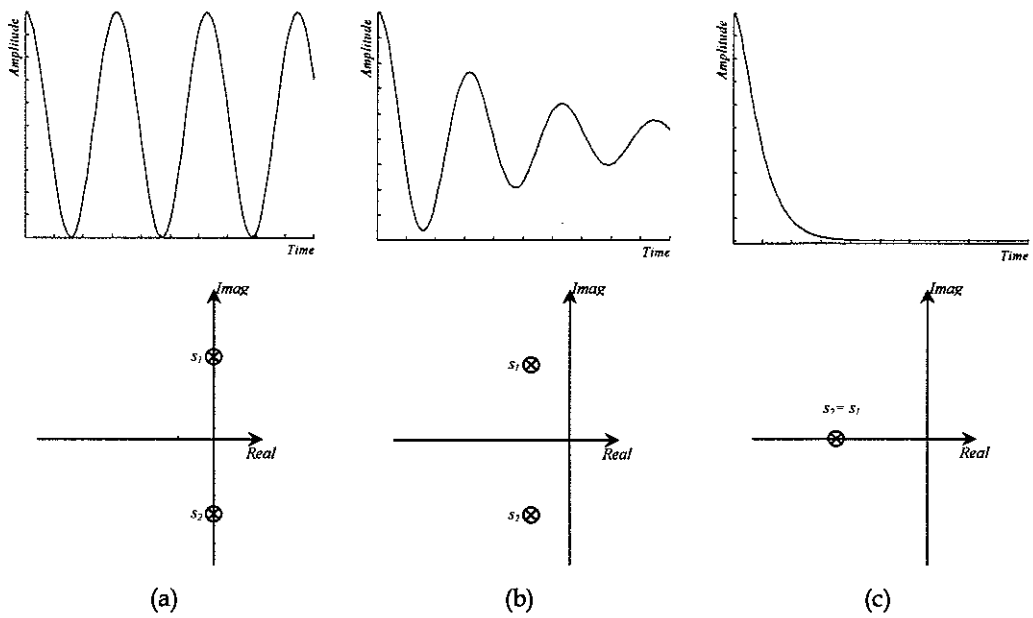

Figure d1.- Roots of the equation 7.7 and their respective free response (a) Both s_1 and s_2 are purely imaginary, (b) s_1 and s_2 are complex conjugates, (c) s_1 and s_2 are real, equal and negative.

Appendix F

Time response curves for the Zener model

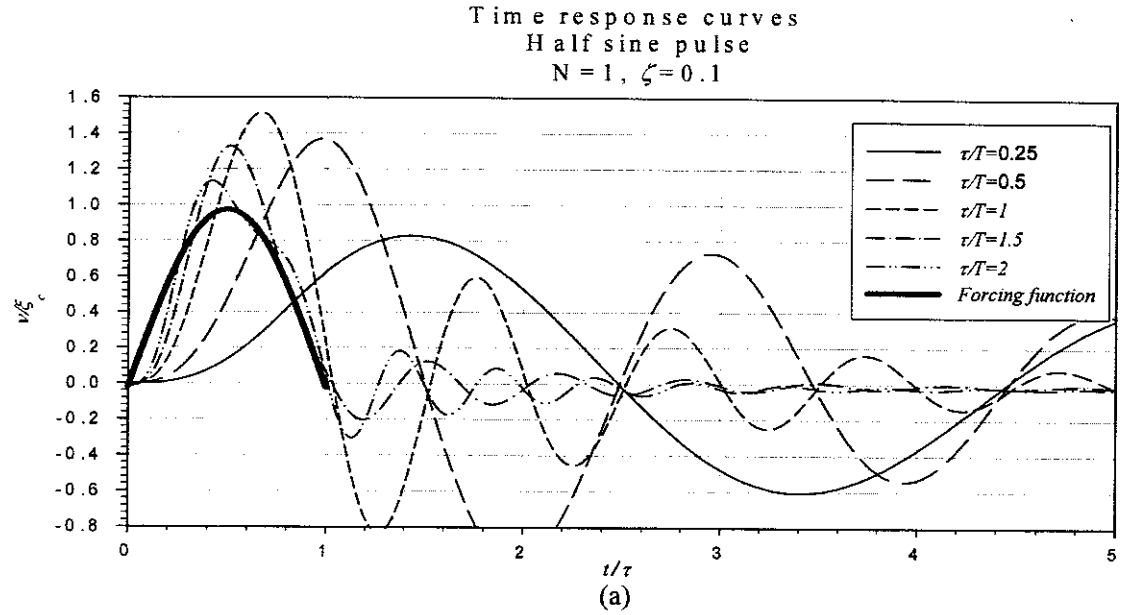

(a)

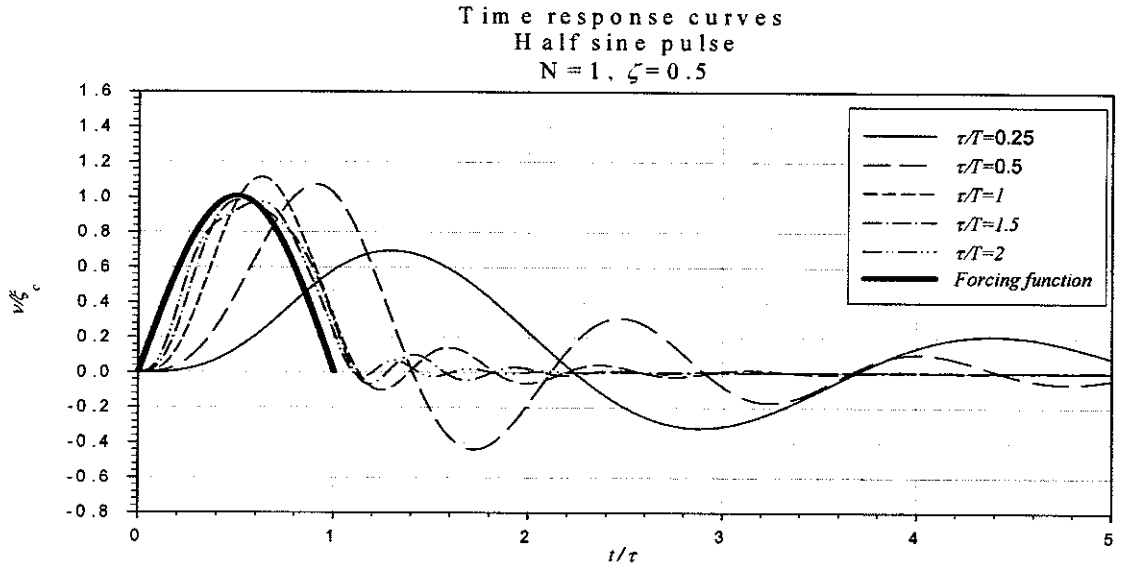

(b)

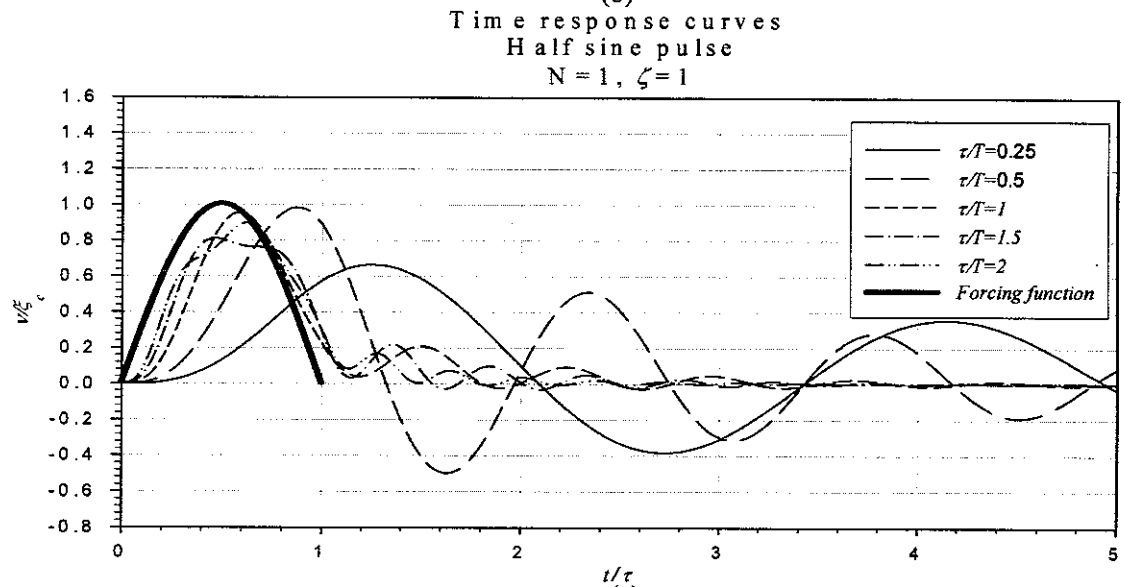

(c)

Time response curves for the Zener model under half sine transient excitation for N=5 and different values of τ/T. (a) ζ=0.1, (b) ζ=0.5, (c) ζ=1

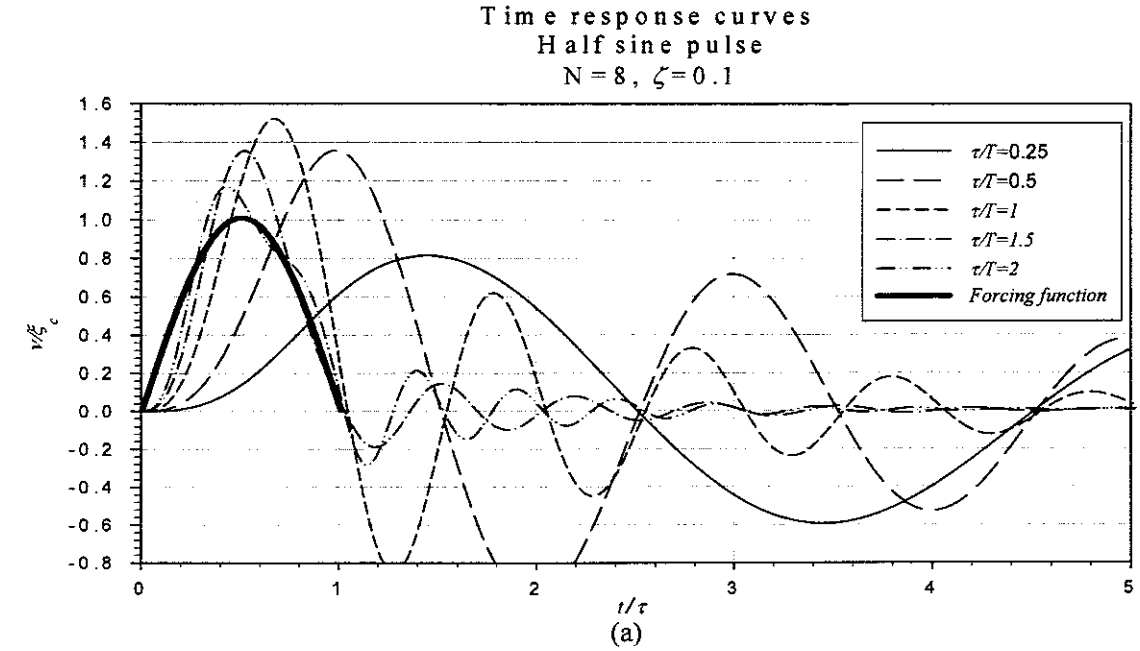

(a)

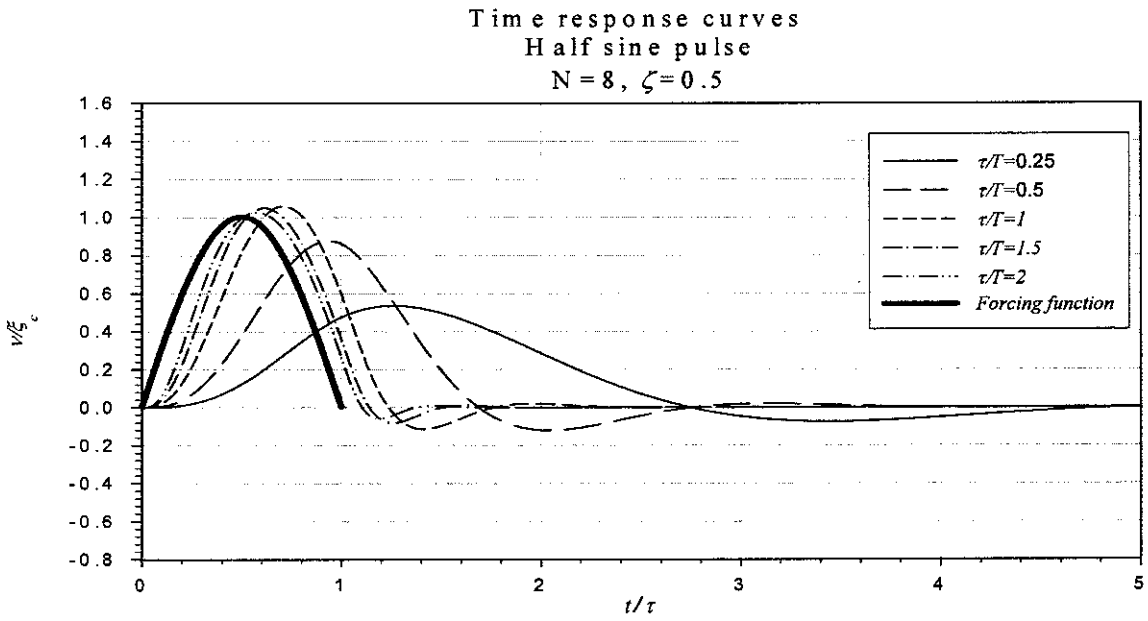

(b)

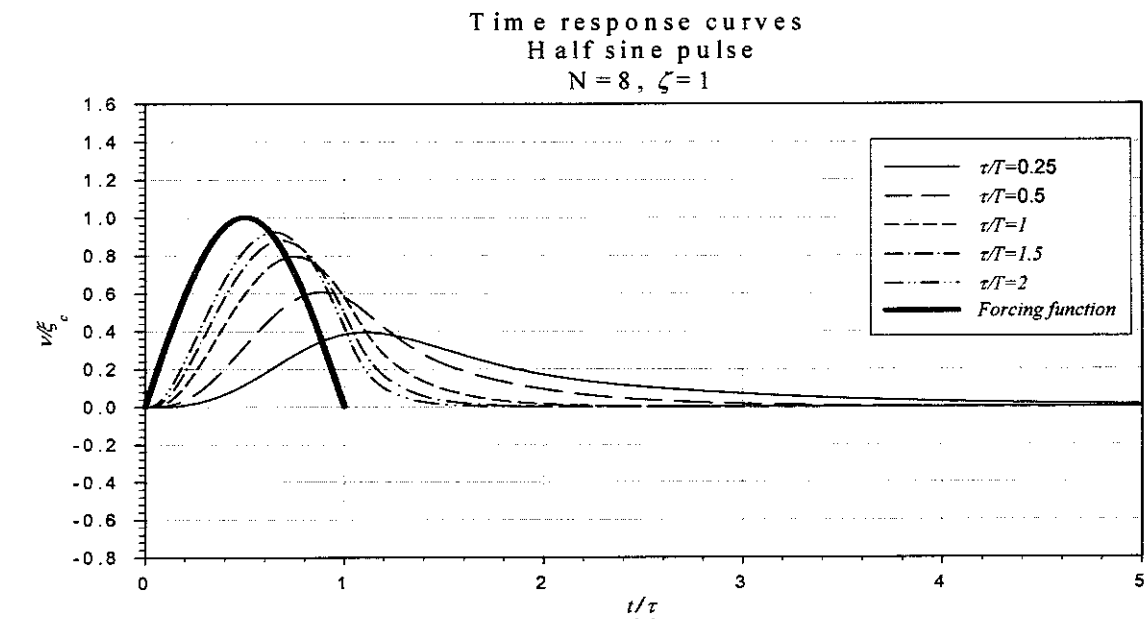

(c)

Time response curves for the Zener model under half sine transient excitation for N=8 and different values of τ/T.
(a) ζ=0.1, (b) ζ=0.5, (c) ζ=1

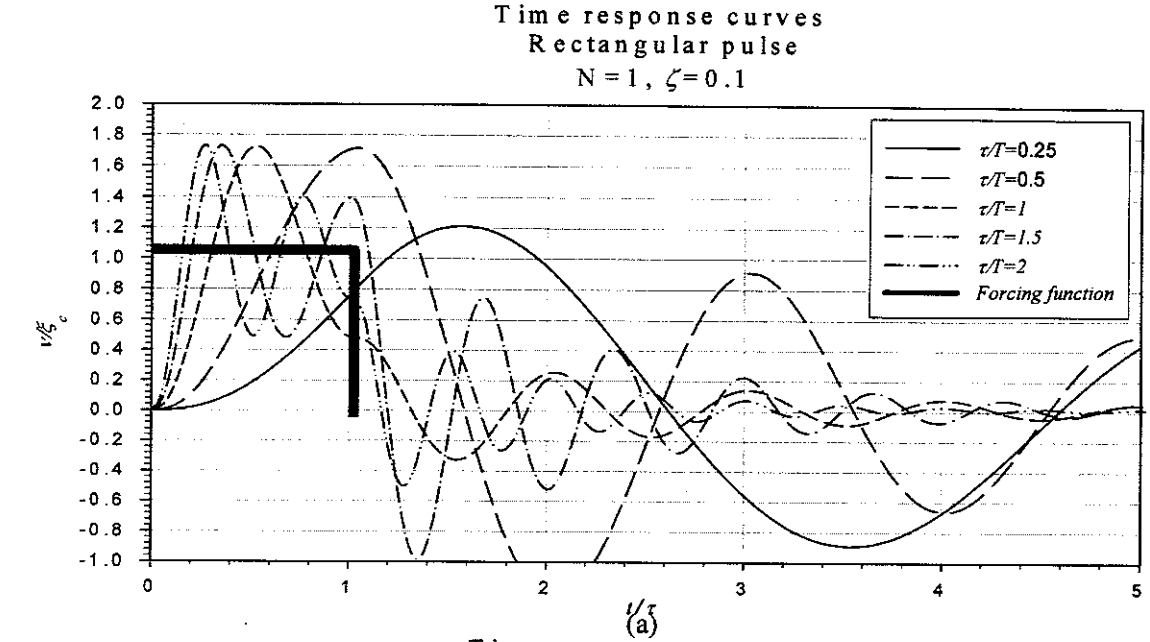

(a)

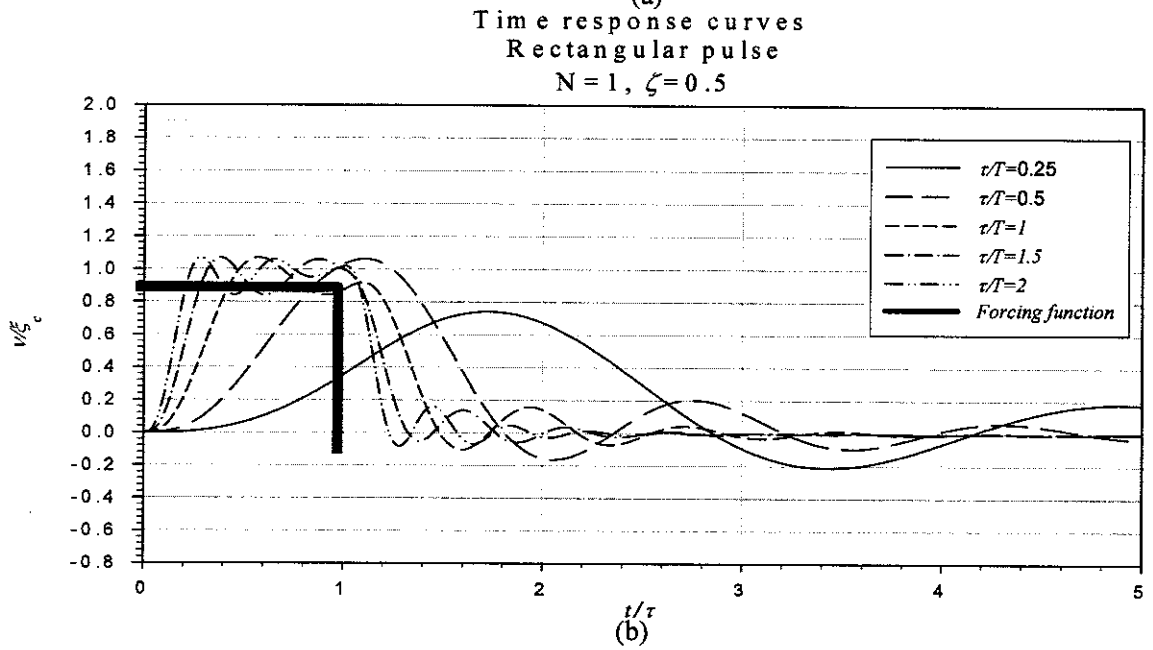

(b)

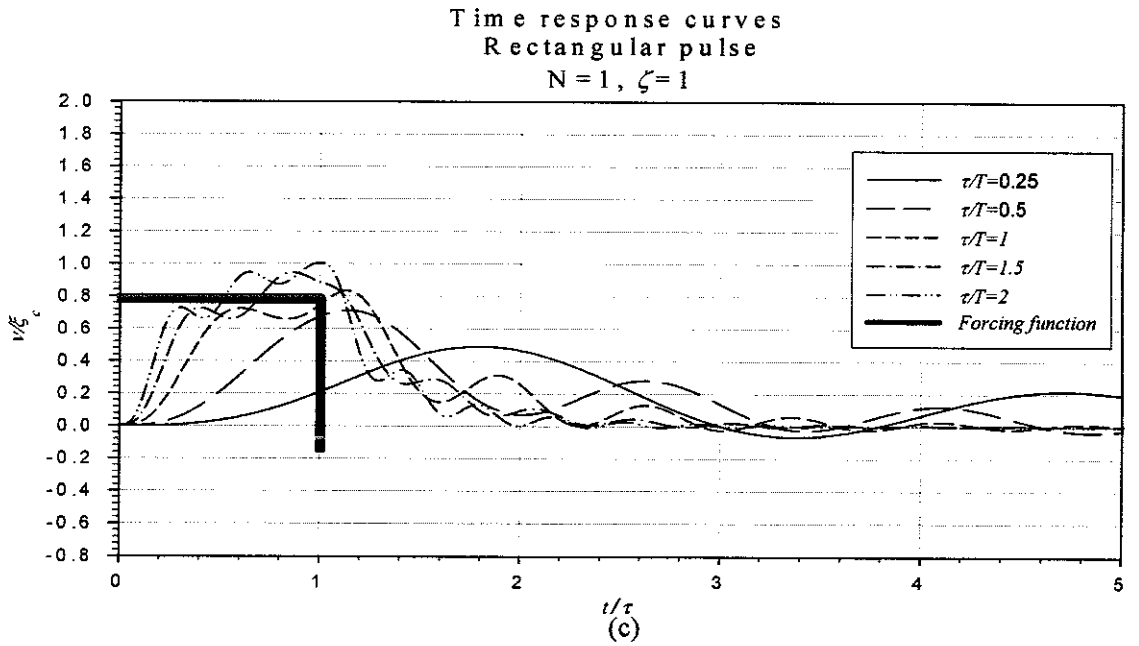

(c)

Time response curves for the Zener model under rectangular transient excitation for N=1 and different values of τ/T. (a) ζ=0.1, (b) ζ=0.5, (c) ζ=1

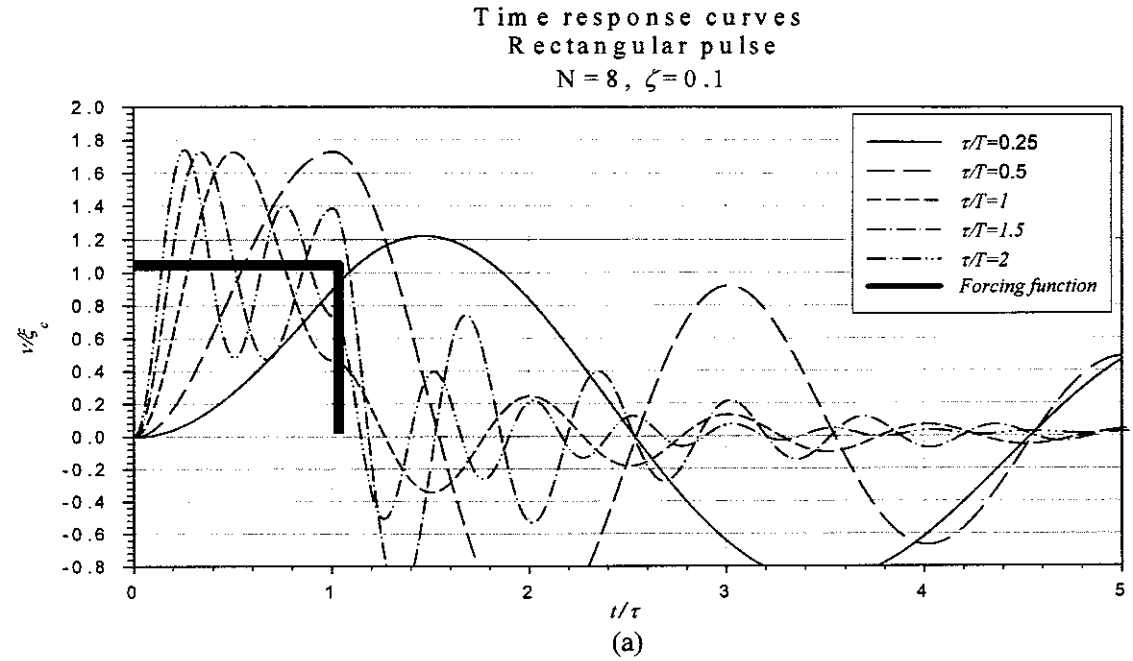

(a)

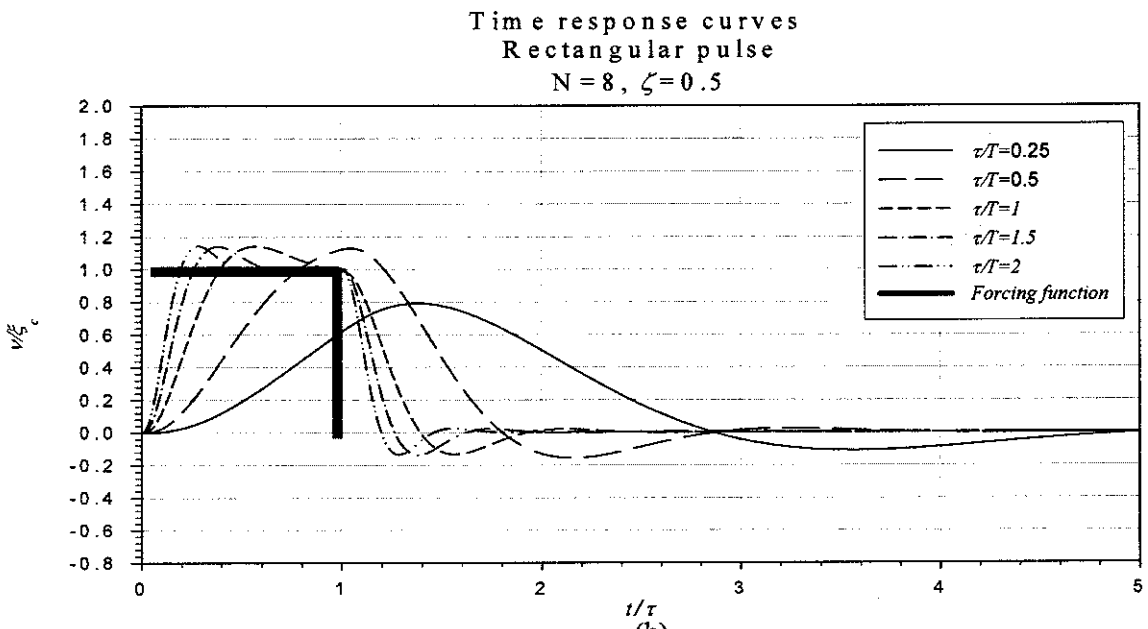

(b)

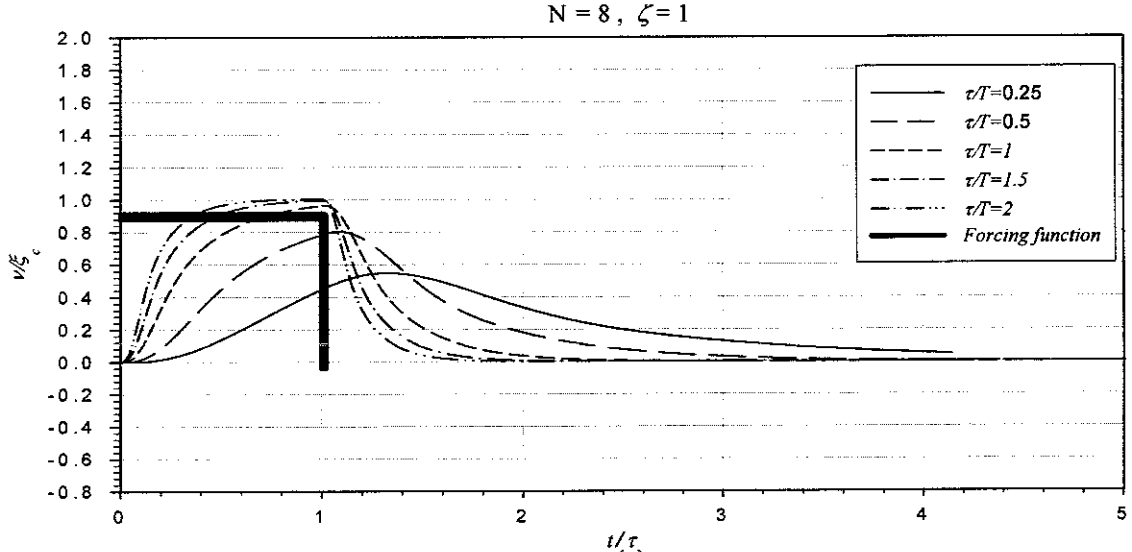

(c)

Time response curves for the Zener model under rectangular transient excitation for N=8 and different values of τ/T.
(a) ζ=0.1, (b) ζ=0.5, (c) ζ=1

References.

1. HARRIS AND CREEDE, 1996: *Shock and vibration handbook,* New York, McGraw-Hill.

2. AYRE, R S, 1958: *Engineering vibrations,* New York, McGraw-Hill.

3. TIMOSHENKO S, YOUNG D H, WEAVER W, 1974: *Vibration problems in engineering,* New York, Wiley and sons.

4. SNOWDON J C, 1968: *Vibration and shock in damped mechanical systems,* New York, Wiley and sons.

5. MORROW C.T, 1963: *Shock and vibration engineering,* New York, Wiley and sons.

6. THOMSON W.T, 1993: *Theory of vibrations with applications,* London, Chapman and Hall.

7. IRWIN J.D, GRAF E.R, 1979: *Industrial noise and vibration control,* New Jersey, Prentice Hall.

8. SKUDRZYK E, 1968: *Simple and complex vibratory systems,* The Pennsylvania State University press.

9. NASHIF A.D, JONES D.I.G, HENDERSON J.P, 1985: *Vibration damping,* New York, Wiley and sons.

10. BERANEK L.L, 1971: *Noise and vibration control,* New York , McGraw-Hill.

11. ZENER C.M, 1948: *Elasticity and anelasticity of metals ,* Chicago, University of Chicago Press.

12. LAKES R.S, 1998: *Viscoelastic solids,* Florida, CRC Press.

13. CLOSE C. M, FREDERICK D.K, 1995: *Modeling and analysis of dynamic systems,* New York, John Wiley and sons.

14. RUZICKA J.E, DERBY T.F, 1971: *Influence of damping in vibration isolation,* US Department of Defence.

15. SNOWDON J C, 1963: Steady state and transient behaviour of two and three element isolation mountings, *The Journal of the Acoustical Society of America,* 35(3) 397-403.

16. CHANDRA N.S, HATWAL H, MALLIK M.K, 1999: Performance of non linear isolators and absorbers to shock excitations, *Journal of Sound and Vibration,* 227(2) 293-307

17. MINDLIN R D : Dynamics of package cushioning, *Bell System Technical Journal,* 24 353-467.

18. MIL-STD-810D, Environmental Test Methods and Engineering Guidelines.

19. CLOSE C. M, FREDERICK D.K, 1995: *Modeling and analysis of dynamic systems,* New York, John Wiley and sons.